Climatic variability over the last 30,000 years recorded in La Piscina de Yuriria, a Central Mexican Crater lake (DOI: 10.1002/jqs.2846)

Jonathan A. Holmes[1*], Sarah E. Metcalfe[2], Heather L. Jones[3], Jim D. Marshall[4].

[1] Environmental Change Research Centre, Department of Geography, University College London, Gower Street, London, WC1E 6BT, UK

[2]School of Geography, University of Nottingham, University Park, Nottingham, NG7 2RD, UK

[3]15 Poppy Close, Southwater, Horsham, RH13 9GW, UK

[4] Department of Earth, Ocean and Ecological Sciences, University of Liverpool, Liverpool, L69 3GP, UK

Corresponding author: Jonathan A. Holmes, j.holmes@ucl.ac.uk

Running head: Palaeolimnology of a Mexican Crater Lake

ABSTRACT: The Trans-Mexican Volcanic Belt provides an excellent setting for reconstruction of late Quaternary climate from different natural archives. Moreover human impact on the landscape since the mid Holocene provides a good opportunity to investigate the complex interplay of natural and anthropogenic forcing of landscape change. However despite the wealth of records, understanding of the environmental history of the region and its wider significance for climate change across the northern neotropics remains incomplete. We present a radiocarbon-dated, multiple-proxy (sedimentology, sedimentary geochemistry, ostracods, diatoms, stable isotopes) record of climatic and environmental change based on the lacustrine sediments from La Piscina de Yuriria, a hydrologically-closed volcanic crater in the northern TMVB. Much of the last glacial interval was characterised by low effective moisture associated with a weakened North American Monsoon (NAM) although the interval from 30,000 to 27,500 aBP experienced abrupt changes in rainfall. The period corresponding to the late glacial stadial was also dry and the lake may have dried out at this time. There was a change to wetter but variable conditions during the early Holocene as the NAM strengthened. Progressive drying during the later Holocene was accompanied by phases of catchment disturbance, which were partly the result of human impact.

Introduction and previous work

The highlands of the Trans-Mexican Volcanic Belt (TMVB), which cross Mexico at around 19°N, provide a range of opportunities for reconstructing past climates through the study of the sediments in its many lake basins, the availability of glacial deposits, tree ring records and a wealth of historical documents (primarily since the Spanish conquest in 1521). In spite of these many possibilities, understanding of climatic variability over the late Quaternary, particularly the late Pleistocene and early Holocene, is still rather limited (Caballero *et al.,* 2010). A number of factors help to explain this, including poor dating control of many records, the effects of tectonic and volcanic activity, and especially human disturbance, which over at least the last 4000 years has had a profound impact on the natural environment to the extent that only records from the highest elevations may be unaffected (e.g. Lozano-Garcia and Vazquez-Selem, 2005). Lake sediment records have dominated studies of central Mexican palaeoclimatology, although recent speleothem records (Bernal *et al.,* 2011) have also made a contribution. Palynology has played a central role in palaeolimnological investigations dating back to the 1950s (Sears and Clisby, 1995; Watts and Bradbury, 1982; Goman and Byrne, 1998; Lozano-Garcia *et al.,* 2005). In this context, the dominance of pine-oak woodlands at higher altitudes in the TMVB has presented further challenges given the limited taxonomic resolution of these pollen types in standard palynology and the impact of long-range dispersal, especially of pine pollen (Correa-Metrio *et al*., 2012). The climatic interpretation of pollen diagrams from the TMVB has often hinged on decisions about the climatic conditions that changing proportions of pine and oak represent, or indeed whether the presence of large percentages of pine means that pine trees were actually present (c.f. Brown, 1985; Park *et al.,* 2010). Pollen records are also highly susceptible to anthropogenic disturbance, although the distinctive presence of *Zea mays* pollen in records is a clear indicator of agricultural activity close to lakes. To help to resolve some of the uncertainties around

75 pollen-based reconstructions, the application of palaeolimnological methods, particularly

76 diatom, geochemical, isotopic and mineralogical analyses, has become increasingly

77 common across the TMVB. Whilst not immune to many of the complicating factors

78 outlined above, this multi-proxy approach has helped to improve our understanding of both

79 climatic and environmental change in this area. In this paper we present a well-dated

80 palaeolimnological record from a crater lake, La Piscina de Yuriria, on the southern edge

81 of the Valle de Santiago region, southern Guanajuato, which extends back some 30,000

82 years (all ages quoted in this paper that relate to the radiocarbon time-span are in

83 calendar years unless otherwise stated). This is considered in the context of other data

84 from adjacent crater lakes in the Valle de Santiago area and other lakes in the wider

85 region to explore the timing and nature of climatic change and human impact.

86

87 The present-day climate of the region, and climate forcing mechanisms over the late

88 Quaternary, are complex. Central Mexico falls under the influence of the North American

89 Monsoon (NAM). Variations in rainfall are forced by northern hemisphere summer

90 insolation over the longer term (millennial timescales) linked to precession, which has

91 caused changes in the position of the inter-tropical convergence zone (ITCZ) (Metcalfe *et*

92 *al.,* 2015). On shorter (centennial and shorter timescales), changes in the Pacific and

93 Atlantic Oceans, both of which are important moisture sources, have influenced rainfall

94 over tropical North America and Central America. During the last glacial and first half of the

95 Holocene, the presence of the Laurentide Ice Sheet influenced the climate of the NAM

96 region. The ice sheet had direct effects, through its impact on the position of the jet stream

97 and the mid-latitude westerly winds, and indirectly via meltwater influx into the Gulf of

98 Mexico, a significant moisture source (Aharon, 2003). As the influence of orbitally-forced

99 summer insolation waned over the course of the Holocene, the effect of other factors such

100 as sea-surface temperature variations in the Pacific and Atlantic, linked to various inter-

101 annual modes of ocean-atmosphere re-organisation, has become increasingly important

102 (Metcalfe *et al.,* 2015).

103

104 **Study Region**

105 La Piscina de Yuriria lies within the Valle de Santiago, which is located at the northern

106 edge of the Michoacán-Guanajuato Volcanic field (Fig. 1), and is distinctive because of the

107 presence of at least seventeen maar type volcanoes, of which a number contained lakes

108 (Aranda Gomez *et al.,* 2013). It lies on the margin of the volcanic uplands to the south and

109 the lowlands of the Rio Lerma, in an area known as the Bajío, which became a very

110 important agricultural region during the Spanish Colonial period (Butzer and Butzer, 1993).

111

112 Seven maar lakes have been identified around the town of Valle de Santiago, of which

113 four contained water in 1900 (Ordonez, 1900). K-Ar dating of some of the maars puts their

114 formation to between 1.2 Ma (Hoya San Nicolas) and 0.07 Ma (Hoya La Alberca).

115 Unfortunately, the maar that contains La Piscina de Yuriria was not dated, although the

116 adjacent shield volcano is believed to date to 6.9 Ma (Aranda-Gomez *et al*., 2013). It has

117 been suggested that these maar lakes were once set within a large palaeolake, which

118 extended from the modern Laguna de Yuriria, northwards around the modern town of

119 Valle de Santiago. The maars have very small catchment areas and the lakes within them

120 were supported by the waters of the underlying Salamanca aquifer. Unfortunately, this

121 aquifer has been heavily exploited (there are more than 1600 active wells), which has

122 resulted in a drawdown of about 2 m yr^{-1} over the past 25 years (Alcocer *et al*., 2000). As

123 a result all the maars are now dry, even those that contained deep lakes in the early

124 1980s. Alcocer *et al.* (2000) report on the many undesirable consequences of this

125 desiccation, including the loss of endemic fish species and lake margin wetland habitats,

126 the economic effect of the loss of fisheries and alkali fly collection and adverse health

127 effects due to the mobilisation of alkaline dust. La Piscina de Yuriria contained a lake

128 approximately 2 m deep in 1981 and was then observed to dry out through the 1980s, with

129 the development of a salt crust across the basin floor. Freshwater springs around the

130 margins of the lake within the crater also dried up. A shallow lake was re-established in

131 the early 1990s, which was then made permanent in the early 2000s by the pumping of

132 groundwater back into the crater. As this was one of the basins where adverse health

133 effects were reported due to dust mobilisation, this re-wetting of the basin may have been

134 a response.

135

136 The Valle de Santiago area lies towards the northern margin of what was the

137 MesoAmerican cultural area in the pre-Hispanic period. There is limited evidence for

138 settlements during the Preclassic period associated with the Chupicuaro culture (ca. 800 –

139 0 BC). Population expanded during the Classic period (ca. AD 300 – 900) when urban

140 centres developed across the Bajío. In the late Postclassic (after ca. AD 1300) the area

141 lay near the frontier between the settled Purépecha (Tarascans) to the south and the

142 nomadic Chichimec to the north (Gorenstein and Pollard, 1983). A church (convento) was

143 built at Yuririapundaro (the Purépecha name for Yuriria) in 1550. The translation of

144 Yuririapundaro is 'Lake of Blood', referring to the distinct red colour of the water in the

145 crater (de Escobar 1729 in Gomez de Orozco, 1972). A similar red colour, probably the

146 result of blooms of sulphur bacteria, was observed at the lake in the 1980s. According to

147 Park *et al.* (2010) the Spanish settled in Valle de Santiago in the early 17th century

148 initiating a period of intensive agricultural exploitation that has lasted until the present day.

149

150 The dramatic effects of water extraction on the maar lakes attracted work on what had

151 been the deep lakes of Hoya la Alberca and the Hoya Rincon de Parangueo (Kienel *et al.,*

152 2009; Park *et al.,* 2010) partly in an effort to retrieve cores of laminated sediments before

153 these became lost through deflation or profoundly disturbed by desiccation and secondary

154 precipitation of evaporite minerals. The Hoya Rincon de Parangueo record goes back to

155 9600 aBP. Prior to this, there had been work on the Hoya San Nicolas (Brown, 1985;

156 Metcalfe *et al.,* 1989), which had been cored in 1979 shortly after it dried out. The basal

157 date on this core was 12,600-12,700 aBP. This maar was re-cored in 2001 with the results

158 reported by Park *et al.* (2010) giving a record believed to extend back to 11,600 aBP (but

159 not directly dated). As described further below, La Piscina de Yuriria was cored in 1981

160 and 1982 prior to its desiccation.

161

162 The interpretation of sequences from the Valle de Santiago maar lakes has been subject

163 to the common uncertainties that affect records from the TMVB region. The interpretation

164 of pine pollen (or the ratio of pine to pine + oak) has been particularly significant here, with

165 Park *et al.* (2010) rejecting Brown's earlier interpretation of wetter conditions between ca.

166 5700 aBP and 3800 aBP in the Hoya San Nicolas. The shallower lakes also seem to have

167 dried up quite regularly through the Holocene, possibly three times in the case of Hoya

168 San Nicolas (Park *et al.,* 2010). The basic framework of change based on these earlier

169 studies seems to be as follows: a cool and relatively moist late glacial (prior to ~12,700

170 aBP); a variable late glacial to Holocene transition; a dry (possibly very dry) early

171 Holocene; the rapid establishment of wetter conditions around 8400 aBP lasting until 5700

172 aBP; dry 5700 – 3800 aBP, then wetter again, but not as wet as the period between

173 around 8400 and 6000 aBP. The late Holocene has been profoundly influenced by human

174 activity with evidence of maize cultivation and enhanced erosion (especially 2200 to 1300

175 aBP). Both Metcalfe *et al.* (1989) and Park *et al.* (2010) report a cessation of human

176 disturbance around 1000 aBP followed by renewed activity after 400 aBP probably

177 associated with Spanish settlement. Our new data from La Piscina de Yuriria allow us

178   both to extend this record back into the last glacial and to test the framework outlined

179   above.

180

181   **Study site**

182   This study is based on lake sediment records from La Piscina de Yuriria (20˚30'N;

183   101˚08'W, 1740 m a.s.l), which is one of the small (area = 0.75 km^2), hydrologically-closed

184   maar lakes in the Valle de Santiago region (Fig. 1). The basaltic basin experiences a

185   subhumid, subtropical climate with annual precipitation of 700-800 mm and supports

186   subtropical thorn bush scrub around the lake and sparse oak woodland above 2200 m

187   a.s.l. (Metcalfe and Hales, 1994; Metcalfe *et al.,* 1994). The lake seems to have been

188   generally shallow in recent times (e.g. ~ 2 m deep in 1981 and 1982, <1 m in 1992, >1.8

189   m in 2004) and has dried up totally in some years (e.g.1989). The lake was saline as a

190   result of evaporative enrichment, as well as highly eutrophic, with an alkalinity/Ca ratio >>1

191   and Na-CO$_3$-Cl-type composition indicating that evaporative evolution occurred along

192   pathway IIIA of Eugster and Hardie (1978). The lake was fed by several circum-neutral to

193   alkaline springs that were fresh to slightly brackish (Table S1) and also of Na-HCO$_3$ type.

194   Evaporative enrichment is also reflected in the limited stable isotope data for the input

195   water (-9.2 ‰) versus lake water (+0.7 ‰) (Table S1). Recent water-level changes have

196   been the result of groundwater extraction for irrigation (e.g. Metcalfe and Hales, 1994) and

197   later artificial recharge; variations during the late Quaternary, which form a major focus of

198   the present study, have largely been driven by changes in effective moisture (precipitation

199   minus evaporation, or P-E), as discussed below.

200

201   **Materials and methods**

202   *Field collection*

7

203 Two lake sediment cores, namely cores YC1 (length 4 m) and YC2 (14.3 m), were

204 recovered from La Piscina de Yuriria from under 2 m of water in 1981 and 1982,

205 respectively, by members of the Tropical Palaeoenvironments Research Group, at the

206 time based at the University of Oxford, UK. Cores were initially wrapped in clingfilm and

207 aluminium foil and stored in plastic tubes at 4°C prior to sectioning into 1 cm slices,

208 typically at 5 cm intervals, for analysis. Some of the data for core YC1 have been

209 published previously (Metcalfe and Hales, 1994; Metcalfe *et al.,* 1994) but are summarised

210 here alongside previously unreported data for that core and for YC2.

211

212 *Physical sedimentology*

213 Sediment samples from YC1 and YC2 were analysed for organic carbon content using

214 loss on ignition at 450 °C, and for carbonate content by calcimetry. Low-frequency

215 magnetic susceptibility was measured using a Bartington MS1 magnetic susceptibility

216 meter.

217

218 *Bulk sediment geochemistry*

219 Dried sediment samples from YC1 were digested using a combination of HNO_3, HF and

220 H_2O_2 following Dean and Gorham (1976). The resulting residue was taken up in dilute HCl

221 prior to analysis of major and minor metals using atomic absorption spectrophotometry

222 (AAS). Samples from YC2 were prepared using the sequential digestion method of

223 Engstrom and Wright (1984) and each separate fraction analyses for major and minor

224 metals as for YC1. However, initial inspection of the results indicated that the fractionation

225 had not worked well for these complex sediments. Consequently, the results for the

226 separated fractions were summed and the data treated as 'bulk' analyses, as for YC1.

227 Only selected metals are reported here, namely Fe, Mn, Al, and K, all of which are

228   abundant in catchment soils and sediments, and so are regarded as good tracers of

229   inwash, as discussed in further detail below.

230

231   *Stable isotopes in endogenic carbonate*

232   Bulk, dried sediment samples from YC1 were sieved through an 80μm mesh to remove

233   shell material, treated with Clorox to remove organic carbon and then dissolved in 100 %

234   phosphoric acid. The evolved CO_2 was then analysed for oxygen and carbon isotopes

235   using a VG 'Micromass' mass spectrometer at the Laboratoire d'Hydrologie et de

236   Géochimie Isotopique, Université de Paris-Sud. Samples from YC2 were prepared in a

237   similar way and analysed using a modified SIRA mass spectrometer at the University of

238   Liverpool. All stable isotope results are reported in standard delta notation relative to the

239   PDB standard.

240

241   As part of the evaluation of the stable isotope results, the mineralogy of the carbonate

242   fractions was assessed by X-ray diffraction using Phillips PW1320/10 and PW1050 X-ray

243   diffractometers. Specifically, the Mg content of calcite was assessed using the method of

244   Goldsmith *et al.* (1961)

245

246   *Ostracods*

247   Bulk sediment samples were disaggregated in ~5 % H_2O_2, sieved through a 63 μm sieve

248   and the coarse fractions used for extraction of ostracod shells under a low-power binocular

249   microscope. Because ostracod abundance varied dramatically, in some samples all of the

250   ostracod valves were picked whereas in richer samples, only the first 350 valves were

251   picked and overall abundance then estimated based on the weight of sediment examined.

252   However, the unpicked fraction of rich samples was inspected for the presence of rare

253   species not identified in the original count. Despite poor ostracod shell preservation in

254   many parts of the core, sufficiently well-preserved valves were found at a number of levels

255   to permit stable-isotope analyses, which were used to complement analyses on the

256   endogenic carbonate.

257

258   Specimens of ostracods from the picked fraction of YC2 were selected and studied

259   carefully for signs of damage, dissolution or replacement. Suitable individuals were then

260   cleaned carefully using a 000 size clean nylon paintbrush and ultra pure deionised water

261   under a binocular microscope to remove surface contaminants. Stable-isotope analyses of

262   multiple shells of *Limnocythere sappaensis* were analysed for oxygen and carbon isotopes

263   using a VG Isocarb coupled to a VG Optima mass spectrometer at the NERC Isotope

264   Geosciences Laboratory, Keyworth (UK). Two samples, composed of up to 8 individual

265   valves, were analyzed at most core levels selected and a weighted mean value for $\delta^{18}O$

266   and $\delta^{13}C$ calculated for plotting purposes.

267

268   *Diatoms*

269   Diatom samples were prepared for analysis at 10 cm intervals in YC1 and 10 – 20 cm

270   intervals (depending on sample availability) in YC2. In YC2, only material from 4 m to the

271   base was sampled in detail after preliminary analysis (samples prepared every 25 – 30

272   cm) had shown that the upper 4 m of the sequence seemed to match well with YC1. Poor

273   valve preservation between 7 m and 12 m meant that the majority of samples were taken

274   below and above this interval. Core samples were complemented by a surface sediment

275   sample and water samples from the lake margin. Samples were treated to remove

276   carbonates and organic matter following the method of Battarbee (1986). In some cases

277   strong acids (H_2SO_4 or HNO_3) were used to break up clumps of sediment. The final

278   suspension was mounted onto coverslips using Naphrax. The same method was used to

279   prepare surface sediment samples. Where possible, 400 valves were counted from each

280   level, although at levels with poor preservation this was sometimes reduced to 100 – 200

281   valves. Identifications were carried out using standard floras including Gasse (1986),

282   Krammer and Lange Bertalot (1988, 1991a and b), Patrick and Reimer (1966, 1975),

283   Schoeman and Archibald (1977). The separation of *Navicula* (*Craticula*) *elkab* from

284   *Craticula halophila* proved to be an important part of the study and is discussed in

285   Metcalfe (1990). The results from YC1 were published in Metcalfe and Hales (1994), and

286   preliminary results from YC2 were described in Park (1999). Diatom results are presented

287   here as percentages of the full counts. Species present at less than 2% and only

288   occurring in one sample are not plotted here.

289

290   Initial zonation was carried out using CONISS, the stratigraphically constrained cluster-

291   analysis program within Tilia (Grimm, 1987). The counts from the core samples were also

292   analysed using CANOCO and TWINSPAN. TWINSPAN (Hill, 1979; Jongman *et al.,* 1992)

293   provided a clustering that was not constrained stratigraphically. CANOCO (ter Braak,

294   1988) was used to explore further the variation between samples and species. The latter

295   analyses were used to determine whether the lake diatom assemblages showed repeat

296   occurrences through time and to explore that trajectory of change.

297

298   *Chronology*

299   Independent chronologies were established using AMS or radiometric radiocarbon dating

300   on bulk organic carbon or carbonate (8 levels were dated from YC1 and 16 from YC2).

301   Lack of appropriate material precluded the dating of terrestrial plant macrofossils from

302   either core, but the absence of carbonate bedrock within the catchment means that

303   hardwater error is unlikely to affect radiocarbon dates at this site. Radiocarbon

304   measurements were performed at the Oxford University Radiocarbon Accelerator Unit,

305   Simon Fraser University Radiocarbon facility, Laboratoire d'Hydrologie et de Géochimie

306   Isotopique, Université de Paris-Sud, the NERC Radiocarbon Facility, East Kilbride and the

307   Arizona AMS Laboratory, University of Arizona. Dates were calibrated using IntCal13

308   (Reimer *et al.,* 2013). For each core, outliers were identified and excluded from

309   subsequent age modeling, which was undertaken using Clam 2.2 (Blaauw, 2010).

310   Although some of the radiocarbon dates have been published previously, we report them

311   again here for the sake of completeness and because we have revised the calibrations.

312

313   **Results**

314   *Chronology*

315   The age model for YC1 is based on 7 of the 8 radiocarbon dates for that core (Table 1,

316   Fig. 2) and the age-depth pairs well described by a 3rd-order polynomial curve. The age

317   model for YC2 is based on 12 of the 16 radiocarbon dates (Table 1, Fig. 2) and the age-

318   depth pairs well described by a 3rd-order polynomial curve. The age models were used to

319   assign ages to each depth within the respective cores. An assessment of the comparability

320   of the independent age models for YC1 and YC2 was also undertaken by comparing

321   variations in their physical sedimentology, which would be expected to change

322   synchronously in the two cores: this assessment is discussed below.

323

324   *Physical sedimentology*

325   Cores YC1 and YC2 core are both composed predominantly of brown to grey,

326   diatomaceous gyttja. In the lower sections of YC2 (at ~26,300, 19,900 and 8300 aBP),

327   centimetre-scale sand layers are present. Desiccation surfaces, represented by sub-

328   vertical fractures infilled with darker material, occur at several depths in the interval

329   between 16,800 and 14,300 and near the top of the sequence (~800 aBP). Nodular,

330   siliceous concretions were observed between the base of the sequence and ~17,500 aBP.

331   The interval 100 – 50 cm (representing ~1100 – 500 aBP) was not recovered in YC2.

332

Organic carbon content, estimated from loss-on-ignition (LOI) at 450˚C, varies between ~9

and 44 % (Fig. 3). From the beginning of the YC2 record until ~14,000 aBP, values

average ~15%, increasing and becoming more variable after this time, with peaks up to 44

%. The LOI record in the upper part of YC2 is well replicated in YC1. Carbonate content

averages around 18 % from the beginning of the record until 14,200 aBP, but with peaks

up to 40 % in places. Between 14,000 and 7800 aBP, carbonate content falls to 14 % and

becomes less variable. From 7800 aBP to the end of the YC2 record, there is a sharp

increase to an average of 33 %, with transient peaks up to 45 %. The pattern of change in

YC1 replicates that in the upper part of YC2, but values are systematically lower.

342

Magnetic susceptibility (χ) values (Fig. 3) are typically lower than 10 x $10^{-7}m^3kg^{-1}$ but with a

number of sharp peaks at several levels and a more gradual increase and then decline

between ~10,100 and 6900 aBP. Values rise sharply at 3600 aBP, after which they remain

high and show increased variability. The pattern of change in YC1 replicates that in the

upper part of YC2.

348

Geochemistry and stable isotopes

Concentrations of K, Fe, Mn and Al are variable throughout the cores. For much of the

lower part of YC2 values are generally low, although there are some transient peaks.

Values typically become higher and more variable after about 5100 aBP in YC2, a pattern

that is generally replicated in YC1. There is strong and statistically-significant correlation

amongst all of the metals discussed here in YC1 and in the section of YC2 covering the

past ~5000 years. Correlations are weaker for the earlier part of YC2 (Table S2).

356

357   Stable isotope values are available for fine-grained carbonates and, for a few levels from

358   YC2 only, for ostracod shells (Fig. 4). Mineralogical determinations showed that the calcite

359   present within the core had low magnesium content (≤4 mole %): nevertheless,

360   appropriate corrections were made to the $\delta^{18}O$ values following Tarutani *et al.* (1969).

361   From the beginning of YC2 to 26,600 aBP, $\delta^{18}O$ and $\delta^{13}C$ values are typically low but

362   variable (from about 0 ‰ to around -11 ‰ and +7.6 to -1 ‰, for $\delta^{18}O$ and $\delta^{13}C$,

363   respectively) and strongly covariant (Fig. 5). Between 25,000 and 14,200 aBP, the stable-

364   isotope values are at relatively low resolution, and typically values are higher than in the

365   preceding interval (up to about +3 ‰ and +8 ‰ for $\delta^{18}O$ and $\delta^{13}C$, respectively) and

366   covariant. Between 10,900 and 6600 aBP, there is a further rise in variability, but $\delta^{18}O$ and

367    $\delta^{13}C$ covary as before. Between 6600 and 4500 aBP, there is a significant shift in the

368   pattern of stable isotope variability, with $\delta^{18}O$ values remaining relatively constant, but $\delta^{13}C$

369   increasing up to +15.4 ‰. After 4500 aBP, $\delta^{18}O$ values vary between about 0 and -2.7 ‰

370   and $\delta^{13}C$ values are markedly reduced compared with the preceding interval. The

371   overlapping sections of YC1 and YC2 show similar patterns of change, especially for $\delta^{13}C$.

372   The low-resolution ostracod values are typically ^{18}O-enriched and ^{13}C-depleted compared

373   with those for fine-grained carbonates.

374

375   *Ostracods*

376   Ostracod abundance varies dramatically, between zero (i.e. barren levels) and ~35,000

377   valves per gram of sediment (Fig. 4). Significant zones of very high abundance are

378   present from the beginning of the YC2 record to until 28,700 aBP and at 21,900 – 21,300

379   aBP, 17,800 – 15,900 aBP, 13,700 – 12,900 aBP, 4800 - 2700 aBP, 2000 – 1100 aBP.

380   Significant zones that are barren or contain very few ostracods occur at 28,500 – 27,800

381   aBP, 19,000 – 18,500 aBP, 15,400 – 14,400 aBP, 10,500 – 8300 aBP, 5300- 4900 aBP.

382   The zones of high abundance generally contain monospecific assemblages of

383 *Limnocythere sappaensis* (both males and females): zones of lower abundance typically

384 support other species as well, including at least one species of candonid, *Heterocypris* sp.,

385 *Physocypria* sp., *Potamocypris* sp., *Strandesia* sp. and *Cypria* sp. Although *L. sappanesis*

386 is regarded as conspecific with *Limnocythere inopinata* (e.g. Martens, 1994), we adopt the

387 name *L. sappaensis* here since this is widely used for the species in North America.

388

389 *Diatoms*

390 The diatom assemblages from surface sediment samples collected in 2 m of water in 1982

391 were dominated by *Navicula (Craticula) elkab* (22%), *N. (C.) halophila* (13%) and a variety

392 of *Nitzschia* species. A sample taken in 1997 in 0.3 m of water, just as a lake was

393 becoming re-established, was dominated by *Anomoeneis sphaerophora* (48%) and

394 *Navicula (Cracticula) elkab* (16%). *Anomoeoneis costata* and *Chaetoceros mulleri* spores

395 made up 8% of the count each (Davies, 2000). A sample taken in 2004, at the edge of the

396 lake, was dominated by *Navicula (Craticula) halophila* (56%), a range of *Nitzschia* species,

397 *Chaetocerous muelleri* (some as resting spores) and *Anomoeoneis sphaerophora* f.

398 *costata* (Hill, 2006), although these each formed less than 6% of the assemblage. In 2004,

399 the lake was hypereutrophic, with TP = 584 µg l^{-1} and chlorophyll-*a* 127 µg l^{-1} (Hill, 2006).

400

401 Preliminary diatom analysis of samples from the top 4 m (past ~5000 years) of the YC2

402 core indicated the presence of similar assemblages to those reported in Metcalfe and

403 Hales (1994), so efforts on this core were focused on the section below 4 m. Here, results

404 are presented from both core sequences (Fig. 6). As with the ostracods, diatom

405 preservation is highly variable through the sequences. In YC2 there was little or no valve

406 preservation between 22,100 – 10,400 aBP cm. In YC1 there are gaps in the record due

407 to poor preservation between 2000 – 1100 aBP. Both sequences are dominated by *N. (C)*

408 *halophila* and *N. (C) elkab*, *A. costata* and *A. sphaerophora*, *C. muelleri* and a range of

409 *Nitzschia* species. These assemblages are all similar to those found in surface sediment

410 samples taken from the lake at different times, reflecting high (if varying) pH and alkalinity,

411 and highly evaporated conditions. A more distinctive aspect of the core records is the

412 abundance, at times, of small *Navicula* species (e.g. *N. fluens*, *N. minusculoides*, *N.*

413 *muralis*).

414

415 **Discussion**

416 We discuss the chronology for the lake-sediment sequences and then the interpretation of

417 each of the palaeolimnological variables, before proceeding to reconstruct the

418 palaeolimnological history of La Piscina de Yuria for the late Quaternary.

419

420 Core YC1 covers the interval from about 4600 aBP to the coring date. The anomalous age

421 at 44-46 cm probably represents inwash of older carbon from the catchment, substantiated

422 by the magnetic susceptibility data. Core YC2 covers the interval from about 31,000 aBP

423 to the coring date. The four dates that are omitted from the age model are all younger than

424 expected, possibly the result of root penetration during times of low lake level. The general

425 pattern of age-depth relationships for YC1 and the upper part of YC2 suggests good

426 agreement between the two cores. Detailed comparisons based on the loss on ignition

427 and magnetic susceptibility profiles (Fig. 2), which would be expected to agree for the two

428 closely-located sequences, suggest a small (~200 years) age offset, with YC2 being

429 consistently older. The fact that small differences exist is perhaps not surprising given that

430 different equivalent depths and contrasting materials were dated in the two cores (Table

431 1). However, rather than correct either one of the cores we prefer to use the age models

432 defined for each respective core and then refer to the resulting uncertainties as

433 appropriate.

434

435   Loss on ignition (LOI) provides a good proxy for the organic carbon content of the

436   sediments (Dean, 1974). The carbon/nitrogen (C/N) ratios (available for YC1 only: data not

437   shown, but values vary between 11.6 and 49.4) indicate that the organic matter is of mixed

438   aquatic and terrestrial sources, suggesting that LOI provides a record of aquatic

439   productivity and terrestrial inwash at least for the past 4,600 years. The $CaCO_3$ content of

440   the sediment is best explained by endogenic carbonate formation within the lake, since the

441   catchment is devoid of carbonate rocks or sediments. In such settings, calcium carbonate

442   precipitates from the water column when the lake becomes saturated with respect to

443   carbon minerals as a result of evaporative enrichment of water or mediated by aquatic

444   plants. However, enhanced aquatic productivity can also lead to carbonate dissolution

445   (e.g. Cohen, 2003) and carbonate formation also depends on supply of ions from the

446   catchment, meaning that the interpretation of sedimentary $CaCO_3$ records is not always

447   straightforward.

448

449   The magnetic susceptibility of the sediments is strongly linked to inwash because the

450   volcanic soils are rich in magnetic minerals. Increases in χ in YC1 have therefore been

451   interpreted as inwash events associated with either natural or anthropogenic catchment

452   disturbance (Metcalfe and Hales, 1994). The elements Fe, Mn, Al and K are all associated

453   with weathered volcanic soils, and their concentrations in the lake sediments are

454   controlled by catchment inwash: Fe and Mn may also have been mediated by redox

455   conditions within the lake although we do not have direct evidence for this.

456

457   The oxygen and carbon isotope composition of lacustrine carbonate is a function of the

458   temperature and isotopic composition of the water in the case of oxygen, and the carbon-

459   isotope composition of dissolved inorganic carbon (DIC) for carbon. In subtropical dryland

460   lakes, such as La Piscina de Yuriria, the oxygen-isotope ratio of lake water is usually the

461 dominant control on the oxygen-isotope composition of carbonate, and this varies with the

462 degree of evaporative enrichment (Talbot, 1990). The carbon-isotope composition of DIC

463 is a complex function of carbon source (catchment- vs lake-derived) and in-lake

464 modification as a result of fractionation during DIC uptake by aquatic plants for

465 photosynthesis, and exchange with atmospheric CO_2 (Talbot, 1990) The same general

466 controls determine the isotopic values of biogenic carbonates, such as ostracod shells, but

467 there may be taxon-specific differences in the exact location and timing (especially

468 season) of carbonate formation compared with endogenic carbonate (e.g. Decrouy *et al.,*

469 2011). Moreover, biogenic carbonate may not be precipitated in isotopic equilibrium with

470 lake water or DIC: ostracod shells, for example, demonstrate offsets from oxygen-isotope

471 equilibrium and are typically ^{18}O-enriched compared with endogenic carbonate

472 precipitated in equilibrium with lake water (von Grafenstein *et al.,* 1999). Further

473 palaeolimnological inferences can be drawn for the strength of covariance amongst

474 carbonate oxygen and carbon isotope values in sediment sequences, strong covariance

475 typically being associated with hydrologically-closed systems (Talbot, 1990).

476

477 Although the occurrence and abundance of different lacustrine ostracod taxa are

478 determined by a range of factors, in La Piscina de Yuriria, salinity, hydrochemistry and the

479 extent to which the lake is seasonally permanent are likely to be the dominant controls. In

480 saline lakes, there is moreover often a relationship between species diversity and ostracod

481 abundance: highly saline lakes are typically dominated by a single species that is present

482 in very high abundance (De Deckker and Forester, 1988).

483

484 Habitat, pH, conductivity, ionic composition and nutrient levels are all major controls on the

485 presence and abundance of diatom species, with some species having well established

486 preferences in relation to some, or all, of these factors (e.g. Gasse, 1986; Kilham *et al.,*

487   1986). In La Piscina de Yuriria, the dominant controls over the full record appear to be

488   those associated with changes in evaporative concentration (pH, EC, ionic composition).

489   NaCl and Na_2CO_3 waters have been shown to be particularly aggressive in relation to

490   diatom dissolution (Barker *et al.,* 1994), so it is likely that some species may be over-

491   represented in the sediment record due to their robust form and heavy silicification. This

492   seems particularly likely in the case of the cysts of *C. muelleri* and may also apply to the

493   more robust forms of species such as *A. costata*, *Denticula elegans* and *Rhopalodia*

494   *gibberula*. Although the impact of differential preservation needs to be borne in mind when

495   interpreting the fossil record, saline-lake diatoms are well established as indirect tracers of

496   climate change (Gasse *et al.,* 1997).

497

498   From the base of YC2, which dates to a little before 30,000 aBP, until around 27,500 aBP,

499   the $\delta^{18}O_{carb}$ record shows marked variability, with the lowest values equivalent to the

500   minimum for the sequence as a whole, and the highest values close to the maximum (Fig.

501   4). There is strong covariance between $\delta^{18}O_{carb}$ and $\delta^{13}C_{carb}$ (Fig. 5) consistent with a

502   hydrologically-closed lake undergoing temporal variations in the degree of evaporative

503   enrichment (Talbot, 1990) in response to changes in effective moisture. The most negative

504    $\delta^{18}O_{carb}$ values equate to un-evolved lake water that was probably fed by springs and

505   rainfall with lower $\delta^{18}O$ than at present ($\delta^{18}O$ around -9 ‰ in summer 1992: Table S1),

506   possibly coupled with cooler conditions. In contrast, the most positive $\delta^{18}O_{carb}$ values in this

507   interval are best explained by evaporative enrichment under reduced effective moisture.

508   The lowest $\delta^{13}C_{carb}$ can be explained by equilibration with atmospheric CO_2 whereas the

509   more positive values require other, or additional, mechanisms to explain them. The uptake

510   of ^{12}C during aquatic photosynthesis by aquatic macrophytes or algae can lead to an

511   increase in the $\delta^{13}C_{DIC}$ and hence of endogenic carbonates, but such an explanation

512   appears inconsistent with low TOC values in this interval (Fig. 3). An alternative

513   explanation is the formation of co-genetic, ^{13}C-enriched, CO_2 during methane formation.

514   Despite the evidence pointing to low lake levels at this time, methane formation in shallow

515   and eutrophic lakes has previously been reported in Mexico (Lake Pátzcuaro: Metcalfe *et*

516   *al.,* 2007) and elsewhere (e.g. Lamb *et al.,* 2000; Gu *et al.,* 2004). The high concentrations

517   of *L. sappaensis* in this interval are consistent with the existence of a saline-alkaline lake

518   (Forester, 1986): interestingly, the peaks in ostracod abundance coincide broadly with the

519   peaks in $\delta^{18}O_{carb}$, suggesting that ostracod numbers increased with salinity, and hence

520   evaporative enrichment. The occurrence of siliceous nodules within the interval,

521   associated with the levels that have the highest $\delta^{18}O_{carb}$ values, is also consistent with the

522   existence of highly saline and alkaline water. The sporadic isotope values from ostracod

523   shells in this interval show ^{18}O-enrichment compared with endogenic carbonates that is

524   broadly consistent with the approximate +0.7 ‰ vital offset recorded for the genus

525   *Limnocythere* (von Grafenstein *et al.,* 1999). In contrast, the carbon isotope values in

526   ostracod shells are similar to those in endogenic carbonate, suggesting that both sources

527   of carbonate precipitated from DIC with a similar $\delta^{13}C$ value once allowance has been

528   made for differences in the timing and exact location of formation. This period covers

529   diatom zones YC2-I and part of YC2-II (Fig. 6). The base of the core is dominated by *C.*

530   *muelleri*, a diatom known to inhabit chloride-rich waters, but the other taxa here do not

531   indicate hypersaline conditions, so it may be over-represented. The most negative $\delta^{18}O_{carb}$

532   value may be reflected in the increase in the freshwater *N. molestiformis* and *N. fluens*

533   although the diatom assemblage overall continues to indicate shallow and alkaline

534   conditions. The presence of *Nitzschia palea* and a form of *Nitzschia frustulum* (both

535   obligate N heterotrophs) also indicates eutrophic conditions, which may help to explain

536   methanogenesis in shallow water conditions (see above). The increasing abundance of *N.*

537   *elkab*, and species of *Anomoeoneis* indicate more consistently high pH (> 8.5) and

538   alkalinity, probably associated with shallowing of the lake. Low magnetic susceptibility and

539 low concentrations of 'inwash' indicator elements (Fe, Mn, K and Al) in this interval

540 suggest that inwash of soil into the lake was limited despite the intervals of increased

541 effective moisture (Fig. 3).

542

543 Between ~27,500 and 14,000 aBP, there was a shift to more positive $\delta^{18}O_{carb}$ and $\delta^{13}C_{carb}$

544 values, although with some stratigraphical variability and strong covariance between

545 $\delta^{18}O_{carb}$ and $\delta^{13}C_{carb}$ (Fig.4, Fig. 5). The elevated $\delta^{18}O_{carb}$ values suggest enhanced

546 evaporative enrichment of lake water under conditions of low effective moisture: the

547 presence of siliceous nodules at various points in this interval support the argument that

548 the lake was shallow, saline and strongly evaporated. Short-term variations in carbonate

549 content also support the occurrence of strong but variable evaporative enrichment (Fig. 3).

550 The presence of multiple surfaces that probably resulted from desiccation in the later part

551 of this interval suggests that lake levels fell and the lake may have dried out totally on

552 several occasions. Elevated $\delta^{13}C_{carb}$ values are too high to be explained solely by

553 equilibration with atmospheric CO_2. Enhanced aquatic productivity, in which ^{12}C-uptake by

554 aquatic plants and algae causes DIC to be enriched in ^{13}C, is incompatible with the low

555 TOC content in this interval: the production of ^{13}C-enriched co-genetic CO_2 in a stagnant,

556 shallow, nutrient-rich lake could provide an alternative explanation as discussed above.

557 From 27,500 to 22,500 aBP, a period of evaporative enrichment and periodic desiccation

558 is consistent with the diatom record for this interval (zones YC2-IIa and YC2-IIb), which

559 ends around 22,500 aBP in a period when diatoms were sparse and poorly preserved

560 (after which there is a break in diatom preservation, see above). There are two notable

561 peaks in *N. minusculoides* reaching 71% of the count between 27,000 and 26,000 aBP

562 and 44% at around 24,000 aBP. The earlier peak is associated with a layer of sand (or

563 tephra, see below) and, moreover, there are no stable isotope data from this layer, so its

564 significance remains unclear. The presence of some freshwater taxa (e.g. *N. fluens*,

565   *Caloneis bacillum*) may reflect fluctuating conditions within a period of overall drying.

566   There are several marked peaks in ostracod abundance during this interval, with

567   assemblages strongly dominated by *Limnocythere sappaensis*, which supports the

568   inference that the lake was generally saline and alkaline. The sporadic occurrence of other

569   taxa suggests the periodic influx of fresher waters: rather than whole-lake freshening,

570   these taxa could indicate surface or subsurface inflow of fresh water at various times. Low

571   magnetic susceptibility values and low concentrations of 'inwash' elements suggest limited

572   transfer of soil or sediment from the catchment during this interval; two sharp peaks in

573   magnetic susceptibility around 26,000 and 23,000 aBP (Fig. 3) may represent tephra,

574   rather than catchment inwash, although this remains to be confirmed.

575

576   There is a gap in the stable isotope record between 14,000 and 11,000 aBP, but evidence

577   for dry conditions during this interval comes from the presence of a desiccation surface

578   and the occurrence of a possible palaeosol. It is also supported by the lack of diatom

579   preservation. Sporadic ostracod occurrence also suggests that the lake may have been

580   ephemeral during this time. This interval covers the northern hemisphere late glacial

581   stadial event and confirms that this was a time of low effective moisture in central Mexico.

582

583   After 11,000 aBP, there was a shift to more negative and also more variable $\delta^{18}O_{carb}$ and

584     $\delta^{13}C_{carb}$ values, consistent with a general increase in effective moisture during the early

585   Holocene (Fig. 4). The rise in magnetic susceptibility, coupled with minor increases in

586   some of the 'inwash' elements, may also reflect enhanced inwash of catchment material

587   during the early Holocene. Diatom preservation resumes (zone YC2-III), with assemblages

588   dominated by *Nitzschia palea* and *Chaetoceros muelleri* (Fig. 6). Assuming that *C.*

589   *muelleri* may be overrepresented, high percentages of *N. palea* and *Nitzschia communis*

590   indicate lower pH and TDS (total dissolved solids) (Gasse, 1986) and eutrophic conditions.

591   This assemblage shows some similarities to that in zone YC2-Ia, but zone YC2-III may

592   represent the period when the lake was freshest and deepest, although not deep enough

593   to develop a truly planktonic flora. Today, assemblages with such high percentages of *N.*

594   *palea* are found in shallow, freshwater lakes in Mexico with high levels of nutrient

595   enrichment such as Lakes Zacapu and Cajititlan (Hill, 2006 and S. Metcalfe, unpublished

596   data). Ostracod concentrations are low, but significantly the assemblages include a

597   relatively high proportion of species other than *L. sappaensis*, consistent with fresher

598   water than in much of the pre-Holocene.

599

600   Between about 8,000 and 4,500 aBP there was a marked change in the lake system.

601   Increase in $\delta^{18}O_{carb}$ values suggests enhanced evaporative enrichment associated with

602   decreased effective moisture (Fig. 4). Most notably, however, is the dramatic positive

603   excursion in $\delta^{13}C_{carb}$ values, up to a maximum of about +16 ‰ and, associated with this,

604   the breakdown in the positive covariance between $\delta^{18}O_{carb}$ and $\delta^{13}C_{carb}$ values that was

605   apparent during earlier intervals (Fig. 5). The very high $\delta^{13}C_{carb}$ values are best explained

606   by methanogenesis, as discussed for earlier intervals above. Interestingly, the single

607     $\delta^{13}C_{ostracod}$ value from this interval does not track the $\delta^{13}C_{carb}$ values, but instead is much

608   lower (Fig. 4). Although we cannot attach too much significance to a single value, this

609   does suggest that the ostracods and the endogenic carbonate were formed in different

610   micro-environments within the lake, or perhaps during different seasons, from DIC with

611   contrasting $\delta^{13}C$ values. Although the $\delta^{18}O_{ostracod}$ values are more positive than the $\delta^{18}O_{carb}$

612   values, as would be expected, the difference is too large to be explained by vital offsets

613   alone, possibly lending support to the view that the endogenic and ostracod carbonates

614   were formed under contrasting conditions or at different times of the year. Ostracods occur

615   sporadically in this interval, indicating that whatever conditions prevailed were not wholly

616   unsuitable for ostracods to live. This period straddles the diatom record at the top of YC2

23

617 (zone YC2-IV) and the bottom of YC1 (zone YC1-I). The diatom assemblage is notable for

618 its dominance by *N. (C.) elkab* and *N. (C.) halophila* (both cores), with *Nitzschia frustulum*

619 and *N. palea* (Fig. 6). The switch to an *N. elkab*/*N. halophila* flora is consistent with a

620 return to more alkaline conditions, probably driven by increasing evaporation. *Navicula*

621 *(C.) elkab* does seem to have a distinct ecology, with a preference for hyper-alkaline,

622 Na_2CO_3 lakes, where Cl^- is also important. *Nitzschia frustulum* tends to be more abundant

623 with *N. (C.) elkab* than with *N. (C.) halophila* (e.g. YC2-4c and base of YC1-1) supporting

624 the interpretation of high alkalinity (Gasse, 1986). Its presence with *N. palea* again seems

625 to indicate high levels of nutrient enrichment. Overall, this assemblage is quite similar to

626 that sampled from the modern lake in 1982, when it was around 2 metres deep. A peak

627 in magnetic susceptibility between about 5,500 and 4,500 BP (Fig. 3) associated with a

628 sharp reduction in $\delta^{18}O_{carb}$ (Fig. 4) points to a climatically-controlled inwash event, which

629 may be reflected by rather poor diatom preservation in YC1.

630

631 After 4,500 aBP, $\delta^{18}O_{carb}$ remained high although with some short-lived negative

632 excursions, whereas $\delta^{13}C_{carb}$ values are reduced dramatically (Fig. 4). For the interval of

633 overlap between YC1 and YC2, there is good agreement between the isotope records,

634 especially so for $\delta^{13}C_{carb}$, once allowance is made for the slight age difference between the

635 two cores, as discussed earlier. There is a large increase in ostracod concentration within

636 much of this interval: the dominance of assemblages by *L. sappaensis*, coupled with the

637 large number of individuals, is consistent with the lake having been saline and alkaline for

638 much of the time (Fig. 4). $\delta^{18}O_{ostracod}$ values are ^{18}O-enriched compared to $\delta^{18}O_{carb}$ values,

639 with the degree of enrichment consistent with vital offsets from oxygen-isotope equilibrium,

640 as discussed above. The $\delta^{13}C_{ostracod}$ values agree well with those for $\delta^{13}C_{carb}$, suggesting

641 that the two sources of carbonate formed under the same set of conditions, as was the

642 case for the interval prior to the positive $\delta^{13}C_{carb}$ excursion. The diatom record for this

643   interval was published by Metcalfe and Hales (1994), although here we plot the data

644   against our new age model (Fig. 6). The species encountered confirm the presence of a

645   shallow alkaline lake throughout the late Holocene, although the balance between CO_3^{2-}

646   and Cl^- seems to have varied. The assemblage in zone YC1-II, for example, may indicate

647   that Cl^- replaced CO_3^{2-} as the dominant anion. The assemblage is similar to Bradbury's

648   (1989) saline marsh group. Fresher conditions were then re-established, associated with

649   inwash from the catchment. This wetter/drier cycle is then repeated in zones YC1-III and

650   YC1-IV. Increasingly hostile conditions for diatom preservation are indicated through zone

651   YC1-V, with only a patchy diatom record between about 2000 and 1200 aBP. It seems

652   likely that the single count available through this period is significantly affected by

653   differential preservation. The diatom record resumes around 1000 aBP with a distinctive,

654   well-preserved sample dominated (55%) by *Navicula muralis* (zone YC1-VII). This diatom

655   is often found on mud flats and amongst aquatic vegetation (Hustedt, 1961-66). When

656   combined with very low magnetic susceptibility values, the diatom assemblages indicate

657   catchment stability. We note that this catchment stability occurs at a time in the late

658   Classic when many sites in the relatively dry parts of Central Mexico were abandoned

659   (Beekman, 2010; Park *et al.,* 2010). The most recent sediments preserve a flora quite

660   similar to that found in the various surface sediment samples, indicating a shallow alkaline

661   lake, but with increasing nutrient levels. The very highly evolved chemistry and rather

662   distinctive diatom flora of La Piscina de Yuriria is described in Davies *et al*. (2002) and

663   sampling in 2003 and 2004 confirmed its hypereutrophic status. Phases of inwash,

664   previously reported in YC1 and attributed to anthropogenic disturbance (Metcalfe *et al.,*

665   1994), are also seen at broadly the same times in YC2, i.e. around 3,600 and 1500 aBP

666   and over the past few centuries. An earlier phase at the base of YC1, which ended in that

667   core around 4700 aBP, appears in its entirety in YC2, starting around 5600 aBP. The

668   absence of *Z. mays* pollen from YC1 during this interval led Metcalfe *et al.* (1994) to

669   suggest that the inwash was climatically-mediated rather than the result of anthropogenic

670   disturbance. For the wider region however, Park *et al.* (2010) suggest that agricultural

671   activity began as early as around 5700 aBP (based on the presence of *Zea* pollen), and

672   expanded around 3000 aBP. Lozano *et al.* (2013) also report the occurrence of *Z. mays*

673   pollen from 3000 aBP in Lake Zirahuen, a lake previously thought to be un-affected by

674   human impact. The main climatic and environmental changes revealed in the records from

675   La Piscina de Yuriria are summarised in Table 2.

676

677   There is a reasonable correspondence between phases of inwash, as indicated by

678   magnetic susceptibility and 'inwash' elements, and intervals of low ostracod abundance for

679   the whole of the Holocene (Fig. 7). This suggests that increased turbidity in the lake, which

680   would likely have arisen during phases of increased inwash, was unfavourable for

681   ostracod survival as has been noted previously (e.g. Bridgwater *et al.,* 1999). Therefore

682   water turbidity is an additional control to hydrochemistry on ostracod assemblages in La

683   Piscina de Yuriria.

684

685   The number of palaeoclimatic records from the TMVB (and indeed the whole of Mexico),

686   extending back to 30,000 BP (Marine Isotope Stage 3) is small and limited to the Basin of

687   Mexico (e.g. Caballero and Ortega-Guerrero, 1998; Roy *et al.,* 2009; Lozano-García *et al.,*

688   2015), Lake Cuitzeo (Israde *et al.,* 2010), Lake Pátzcuaro (Watts and Bradbury, 1982;

689   Bradbury 2000) and Lake Zacapu (Correa-Metrio *et al.,* 2012). Moreover, most of these

690   have limited dating control for the older sediments. Caballero *et al.* (2010) integrated

691   palaeolimnological records with evidence from glacial chronologies (Vazquez Selem and

692   Heine, 2004) to provide a palaeoclimatic scenario for the period from around 30,000 aBP

693   to the last glacial maximum (LGM). A more recent consideration of the record from Lake

694   Chalco in the Basin of Mexico has been published by Lozano-Garcia *et al.* (2015). With

695 the exception of Lake Pátzcuaro (one of the westernmost sites), the records suggest

696 drying and cooling after about 30,000 aBP, with glacial advances restricted until around

697 22,000 aBP. The data from La Piscina de Yuriria suggest that there were rapid shifts

698 between wet and dry conditions during this interval, with a general drying trend sometime

699 between about 27,500 and 25,000 aBP. However, the relatively low resolution of the

700 record after about 27,500 aBP means that a continuation of abrupt shifts in rainfall cannot

701 be ruled out. Major glacial advances in the TMVB occurred around the LGM (22,000 –

702 18,000 aBP) with a suggested $6 – 8^{o}C$ lowering in mean annual temperature. Reduced

703 temperature, along with low effective moisture, could have contributed to the elevated

704 $\delta^{18}O_{carb}$ values at this time. Although generally dry, there seem to have been short lived

705 lake highstands in Cuitzeo and rising water levels in the Chalco Basin (southern Basin of

706 Mexico) and the Lerma Basin around 18,000 and 19,000 aBP respectively (Caballero *et*

707 *al.*, 2002). Unfortunately the evidence from La Piscina de Yuriria is at too low resolution to

708 be able to detect these highstands. The late glacial in the TMVB (18,000 – 15,000 aBP) is

709 described as cold and dry, with minor glacial recession (Caballero *et al.,* 2010): evidence

710 from La Piscina de Yuriria indicates a continuation of dry conditions through the late glacial

711 (=Younger Dryas) stadial. Significant warming and glacial retreat apparently started

712 around 14,000 aBP.

713

714 Overall, the records of cool and dry conditions around the LGM and into the early

715 Holocene from the central and eastern part of the TMVB are most easily explained by a

716 reduction in summer season precipitation, which is driven today by the northward

717 movement of the ITCZ and the onset of the NAM. Records from the Pátzcuaro Basin, to

718 the west of this group, show high lake levels persisting through the LGM (Bradbury 2000;

719 Metcalfe *et al.,* 2007), while Correa-Metrio *et al.* (2012) suggest conditions moist enough

720 for pine forest to dominate over grasslands in the Zacapu basin. In both cases an increase

in winter precipitation may provide an explanation although it is hard to reconcile this with the stable-isotope data from La Piscina de Yuriria, which suggest an overall decrease in effective moisture. Lachniet *et al.* (2013) have further suggested that the summer monsoon did not collapse during the last glacial, although once again the evidence from La Piscina de Yuriria does not appear to support this, nor does the latest interpretation of the Chalco record (Lozano-Garcia *et al.,* 2015). The late glacial stadial was a time of dry conditions, with some suggestion that La Piscina de Yuriria may have dried out. A dry Younger Dryas stadial has also been reported from Zacapu (Correa-Metrio *et al.,* 2012) and from sites in northern Mexico (e.g. Roy *et al.,* 2013). Interestingly, the Younger Dryas is also reported as dry in the Juxtlahuaca speleothem record (Lachniet *et al.,* 2013) where it is attributed to monsoon collapse. It appears that the weakening of the Atlantic Meridional circulation (AMOC), the subsequent southward displacement of the ITCZ and a weaker monsoon led to dry conditions over the northern hemisphere neotropics (Bush and Metcalfe, 2012). Only at the northern edge of the NAM region did the resumption of cold conditions allow more penetration of mid-latitude westerlies leading to wetter conditions (Metcalfe *et al.,* 2015).

The classic pattern of climatic change in the NH tropics and subtropics is for wetter conditions in the early Holocene driven by poleward migration of the ITCZ and a stronger monsoon in response to insolation forcing. Whilst there is some support from this in Mexico, it seems that the establishment of the modern climatic regime was delayed by the presence of the residual Laurentide Ice Sheet and the influence of meltwater pulses entering the Gulf of Mexico (Metcalfe *et al.,* 2015). The early Holocene interval in La Piscina de Yuriria indicates a change to wetter conditions overall, but with evidence for abrupt shifts between wet and dry conditions. A similar pattern is recorded by Park *et al.* (2010) for their other sites in the Valle de Santiago. The response of the wider NAM region

747   to the insolation maximum in the early Holocene is complex, with the clearest response in

748   the south, where the direct influence of the ITCZ is strongest. Elsewhere, it seems that the

749   modern NAM regime may not have resumed until after 8000 aBP and there was a trade-

750   off between increasing precipitation and increasing temperatures (Metcalfe *et al.,* 2015).

751   La Piscina de Yuriria shows an overall trend of drying from the mid Holocene onwards.

752   This is consistent with the southward migration of the ITCZ and as the role of insolation

753   forcing became weaker, so the effect of other climate forcings such as ENSO, seems to

754   have become more important giving rise to increasingly complex patterns of change. This

755   drying was accompanied by increasing human impact, as shown by evidence for phases

756   of sediment inwash and by the presence of *Z. mays* pollen. Increasing human impact

757   during this interval is also evident from other sites in Mexico (Metcalfe *et al.,* 1994).

758

759   **Conclusions**

760   In summary, evidence from La Piscina de Yuriria indicates that the climate of Central

761   Mexican highlands has changed dramatically over the past ~30,000 years. Between

762   30,000 and about 27,500 aBP it was highly variable with shifts, which may have been

763   abrupt, between dry and wet conditions. Over much of the glacial period, from ~27,500 to

764   about 14,000 aBP, climate became drier: there may have been abrupt shifts during this

765   interval, but the low resolution of our data means that any such shifts are not revealed.

766   The occurrence of strong millennial scale variability during MIS3, with a global signature,

767   has been widely noted (Clement and Peterson, 2008), apparently driven by changes in

768   AMOC. It is notable that there were three D/O warming events (2 – 4) between 30,000 and

769   22,000 aBP (Wolff et al., 2010) and two Heinrich events (H2 and H3). Modelling has

770   indicated differential sensitivity of AMOC under MIS3 and LGM conditions (e.g. Van

771   Meerbeeck et al. 2009), with the climate becoming less sensitive to AMOC changes as the

772   full glacial climate was established. The growth of the Laurentide Ice sheet from an

773 interstadial minimum around 35,000 aBP to its maximum by ca. 25,000 aBP (where it

774 remained until around 15,000 aBP) (Dyke et al., 2002) also reflects the shift of the global

775 climate system into full glacial mode, where other, less rapid forcings may have dominated

776 (see Baker and Fritz, 2015). There is evidence of drought during the period that

777 encompassed the late glacial stadial. During the Holocene, the climate initially became

778 wetter, although the positive water balance was insufficient to lead to major changes in the

779 lake's chemistry and diatom flora. A fall in lake levels under drier climate in the mid

780 Holocene was accompanied by a change in limnology that caused methane formation.

781 Inwash of catchment soils and sediments was the result of a combination of natural

782 climatic triggers and, for the later Holocene, anthropogenic disturbance.

783

798

799

References

800

801 Aharon P. 2003. Meltwater flooding events in the Gulf of Mexico revisited: implications for

802 rapid climate changes during the last deglaciation. *Paleoceanography,* **18:** 1079,

803 doi:10.1029/2002PA000840

804

805 Alcocer J, Escobar E, Lugo A. 2000. Water use (and abuse) and its effects on the crater-

806 lakes of Valle de Santiago, Mexico. *Lakes & Reservoirs: Research & Management,*

807 **5:** 145–149.

808

809 Aranda-Gómez JJ, Levresse G, *et al.* 2013, Active sinking at the bottom of the Rincón de

810 Parangueo Maar (Guanajuato, México) and its probable relation with subsidence faults at

811 Salamanca and Celaya. *Boletín de la Sociedad Geológica Mexicana,* **65:** 169-188.

812

813 Baker PA, Fritz SC. 2015. Nature and causes of Quaternary climate variation of tropical

814 South America. *Quaternary Science Reviews,* **124**: 31-47.

815

816 Barker P, Fontes J-C, Gasse F, Druart JC. 1994. Experimental dissolution of diatom silica

817 in concentrated salt solutions and implications for palaeoenvironmental reconstruction.

818 *Limnology and Oceanography,* **39:** 99-110.

819

820 Battarbee, R.W. 1986. Diatom Analysis. In*: Handbook of Holocene Palaeoecology and*

821 *Palaeohydrology* [Berglund BE, (Ed.)] John Wiley & Sons Ltd: New York; pp. 527-570.

822

823 Beekman CS. 2010. Recent research in Western Mexican archaeology. *Journal of*

824 *Archaeological Research* **18:** 41-109.

825

826   Bernal JP, Lachniet M, McCulloch M, Mortimer G, Morales P, Cienfuegos E. 2011. A

827   speleothem record of Holocene climate variability from southwestern Mexico. *Quaternary*

828   *Research,* **75:** 104-113

829

830   Blaauw M. 2010. Methods and code for 'classical' age-modelling of radiocarbon

831   sequences. *Quaternary Geochronology,* **5:** 512-518.

832

833   Bradbury JP. 1989. Late Quaternary lacustrine paleoenvironments in the Cuenca de

834   Mexico. *Quaternary Science Reviews*, **8**: 75-100.

835

836   Bradbury JP. 2000 Limnologic history of Lago de Pátzcuaro, Michoacán, Mexico for the

837   past 48,000 years: impacts of climate and man. *Palaeogeography Palaeoclimatology*

838   *Palaeoecology* **63:** 169-195.

839

840   Bridgwater ND, Heaton THE, O'Hara SL. 1999. A late Holocene palaeolimnological record

841   from central Mexico, based on faunal and stable-isotope analysis of ostracod shells.

842   *Journal of Paleolimnology*, **22**: 383-397.

843

844   Brown RB. 1985. A summary of Late-Quaternary pollen records from Mexico west of the

845   Isthmus of Tehuantepec. In: *Pollen Records of Late Quaternary North American*

846   *Sediments.* [Bryant VM, Holloway RG. (Eds.)]. American Association of Stratigraphic

847   Palynologists: Dallas; pp. 71-92.

848

849 Bush MB, Metcalfe SE, 2012 Latin America and the Caribbean. In: *Quaternary*

850 *Environmental Change in the Tropics.* [Metcalfe SE, Nash DJ. (Eds)]. J. Wiley & Sons:

851 Chichester; pp. 263-311.

852

853 Butzer K, Butzer, EK. 1993. The sixteenth-century environment of the Central Bajio:

854 Archival reconstruction from Colonial land grants and the question of Spanish ecological

855 impact In: *Culture, Form and Place*. [Mathewson K. (Ed.)] Baton Rouge, LA, *Geoscience*

856 *and Man* **32:** pp. 89-124.

857

858 Caballero M, Ortega-Guerrero B. 1998. Lake levels since 40,000 years ago at Chalco

859 Lake, near Mexico City. *Quaternary Research,* **50:** 90-106.

860

861 Caballero, M, Ortega, B, Valadéz, F, Metcalfe, S, Macías, J, Sugiura, Y. 2002. Sta. Cruz

862 Atizapan: a 22-ka lake level record and climatic implications for the late Holocene human

863 occupation in the upper Lerma Basin. *Palaeogeography, Palaeoclimatology,*

864 *Palaeoecology,* **186:** 217-235.

865

866 Caballero M, Lozano-García S, Vázquez-Selem L, Ortega B. 2010. Evidencias de cambio

867 climático y ambiental en registros glaciales y en cuencas lacustres del centro de México

868 durante el último máximo glacial. *Boletín de la Sociedad Geológica Mexicana,* **62:** 359-

869 377.

870

871 Clement AC, Peterson LC. 2008. Mechanisms of abrupt climate change of the last glacial

872 period. *Reviews of Geophysics*, **46**, RG4002/2008.

873

874 Cohen AS. 2003. *Paleolimnology: the history and evolution of lake systems.* Oxford

875 University Press: New York; 528 pp.

876

877 Correa-Metrio A, Lozano-Garcia S, Xelhuantzi-Lopez S, Sosa-Najera S, Metcalfe SE.

878 2012. Vegetation in western Central Mexico during the last 50,000 years: modern analogs

879 and climate in the Zacapu Basin. *Journal of Quaternary Science,* **27**: 509-518.

880

881 Davies HL. 1995. *Quaternary Palaeolimnology of a Mexican Crater Lake.* Unpublished

882 PhD thesis, Kingston University.

883

884 Davies SJ. 2000. *Environmental change in the west-central Mexican highlands over the*

885 *last 1,000 years: evidence from lake sediments.* Unpublished PhD thesis, University of

886 Edinburgh.

887

888 Davies, SJ, Metcalfe, SE, Caballero, ME, Juggins, S. 2002. Developing diatom-based

889 transfer functions for Central Mexican lakes. *Hydrobiologia,* **467**: 199-213.

890

891 De Deckker P, Forester RM. 1988. The use of ostracods to reconstruct

892 palaeoenvironmental records. In: *Ostracods in the Earth Sciences*. [De Deckker P, Colin J-

893 P, Peypouquet, J-P. (Eds.)] Elsevier: Amsterdam; pp.175-199.

894

895 Dean, W.E. 1974. Determination of carbonate and organic matter in calcareous sediments

896 and sedimentary rocks by loss of ignition: comparison with other methods. *Journal of*

897 *Sedimentary Petrology*. **44:** 242-248.

898

899　Dean WE, Gorham E. 1976. Major chemical and mineral components of profundal surface

900　sediments in Minnesota lakes. *Limnology and Oceanography,* **21:** 259-284.

901

902　Decrouy L, Vennemann TW, Ariztegui D. 2011. Controls on ostracod valve geochemistry,

903　Part 1: variations of environmental parameters in ostracod (micro-) habitats. *Geochimica et*

904　*Cosmochimica Acta*, **75**: 7364–7379.

905　Dyke AS, Andrews JT, Clark PU, England JH, Miller GH,Shaw J, Veillette JJ. 2002. The

906　Laurentide and Innuitian ice sheets during the Last Glacial Maximum. Quaternary Science

907　Reviews **21:** 9-31.

908

909　Engstrom DR, Wright HEJ. 1984. Chemical stratigraphy of lake sediments as a record of

910　environmental change. In: *Lake Sediments and Environmental History*. [Haworth Y, Lund

911　E. (Eds.)]. Leicester University Press: Leicester; pp. 11-67.

912

913　Eugster HP, Hardie LA. 1978. Saline Lakes. In: *Lakes: Chemistry, Geology, Physics.*

914　[Lerman A. (Ed.)]. Springer-Verlag: New York; pp. 237–294.

915

916　Forester RM. 1986. Determination of the dissolved anion composition of ancient lakes

917　from fossil ostracodes. *Geology*, **14**: 796-798.

918

919　Gasse, F., 1986. East African Diatoms. Taxonomy, ecological distribution. *Bibliotheca*

920　*Diatomologica.* **11:** J. Cramer: Stuttgart; 202 pp.

921

922　Gasse F, Barker P, Gell PA, Fritz SC, Chalié, F. 1997. Diatom-inferred salinity in

923　palaeolakes: an indirect tracer of climate change. *Quaternary Science Reviews*, **16:** 547-

924　563.

925

926 Goldsmith JR, Graf DL, and Heard HC. 1961. Lattice Constants of the Calcium-

927 Magnesium Carbonates. *American Mineralogist,* **43:** 84-101.

928

929 Goman M, Byrne R. 1998. A 5000-year record of agriculture and tropical forest clearance

930 in the Tuxtlas, Veracruz, Mexico. *The Holocene* **8:** 83-89.

931

932 Gomez de Orozco, F. 1972. *Cronícas de Michoacán.* UNAM: Mexico; 214 pp.

933

934 Gorenstein S, Pollard HP. 1983. The Tarascan civilisation: a late Prehispanic cultural

935 system. *Publications in Anthropology* **28:** Vanderbilt University Press, Nashville,

936 Tennessee. 199 pp.

937

938 Grimm EC. 1987. CONISS: a FORTRAN 77 program for stratigraphically constrained

939 cluster analysis by the method of incremental sum of squares. Computers and

940 Geoscience, **13:** 13-35

941

942 Gu B, Schelske CL, Hodell DA. 2004. Extreme ^{13}C enrichment in a shallow hypereutrophic

943 lake: implications for carbon cycling. *Limnology and Oceanography,* **49:** 1152–1159.

944

945 Hill MO. 1979. TWINSPAN: A FORTRAN program for arranging multivariate data in an

946 ordered two-way table by classification of the individuals and attributes. *Ecology and*

947 *Systematics,* Cornell University: New York; 48 pp.

948

949 Hill E. 2006. *Quantitative reconstruction of eutrophication histories in Central Mexican*

950 *lakes.* Unpublished PhD thesis, University of Nottingham.

951

952   Hustedt, F., 1961-1966. *Die Kieselalgen Deutschlands, Österreichs und der Schweiz,* **Vol.**

953   **3.** Reprinted 1977, Otto Koeltz: Koenigstein; 816 pp.

954

955   Israde Alcántara I, Velázquez-Duran R, Lozano García MS, Bischoff J, Dominquez

956   Vázquez G, Garduño Monroy VH. 2010. Evolución paleolimnológica del Lago Cuitzeo,

957   Michoacán durante el Pleistoceno-Holoceno. *Boletin de la Sociedada Geologica*

958   *Mexicana,* **62:** 345-357.

959

960   Jongman RHG, ter Braak CJF, Van Tongeren OFR (Eds.) 1992. *Data Analysis in*

961   *Community Ecology and Landscape Ecology*. Cambridge University Press: Cambridge;

962   324 pp.

963

964   Kienel U, Wulf Bowen S, Byrne R, Park J, Bohnel H, Dulski P, Luhr JF, Siebert   L, Haug

965   GH, Negendank JFW, 2009. First lacustrine varve chronologies from Mexico: impact of

966   droughts, ENSO and human activity since AD 1840 as recorded in maar sediments from

967   Valle de Santiago. *Journal of Paleolimnology,* **42:** 587-609.

968

969   Kilham P, Kilham SS, Hecky RE. 1986. Hypothesized resource relationships among

970   African planktonic diatoms. *Limnology and Oceanography,* **31:** 1169-1181.

971

972   Krammer K. Lange-Bertalot H. 1988. *Süsswasserflora von Mitteleuropa.*

973   *Bacillariophyceae. 2. Teil: Epithemiaceae, Bacillariaceae, Surirellaceae.* Vol. 2/2. Gustav

974   Fischer Verlag: Stuttgart; 596 pp.

975

976 Krammer K. Lange-Bertalot H. 1991a. *Süsswasserflora von Mitteleuropa.*

977 *Bacillariophyceae. 3. Teil: Centrales; Fragilariaceae, Eunotiaceae.* Vol. 2/3. Gustav

978 Fischer Verlag: Stuttgart; 576 pp.

979

980 Krammer K. Lange-Bertalot H. 1991b. *Süsswasserflora von Mitteleuropa.*

981 *Bacillariophyceae. 4. Teil: Achnanthaceae.* Vol. 2/4. Gustav Fischer Verlag: Stuttgart; 437

982 pp.

983

984 Lachniet MS, Asmerom Y, Bernal JP, Polyak VJ, Vazquez-Selem L. 2013. Orbital pacing

985 and ocean circulation-induced collapses of the Mesoamerican monsoon over the past

986 22,000 y. *Proceedings of the National Academy of Sciences,* **110:** 9255-9260.

987

988 Lamb AL, Leng MJ, Lamb HF, Ummer M. 2000. A 9000-year oxygen and carbon isotope

989 record of hydrological change in a small Ethiopian crater lake. *The Holocene,* **10:** 167-177.

990

991 Lozano-García S, Vázquez-Selem L. 2005. A high-elevation Holocene pollen record from

992 Iztaccíhuatl volcano, central Mexico. *The Holocene,* **15:** 329-338.

993

994 Lozano-García, S., Sosa-Nájera, S., Sugiura, Y. and Caballero, M. 2005. 23,000 yr of

995 vegetation history of the Upper Lerma, a tropical high-altitude basin in Central Mexico.

996 *Quaternary Research* 64, 70-82.

997

998 Lozano-Garcia S, Torres-Rodríguez E, Ortega B, Vázquez G, Caballero M. 2013.

999 Ecosystem responses to climate and disturbances in western central Mexico during the

1000 late Pleistocene and Holocene. *Palaeogeography Palaeoclimatologyy Palaeoecology,*

1001 **370:** 184-195.

1002

1003   Lozano-Garcia S, Ortega B., Roy P, Beramendi-Orosco L, Caballero, M. 2015. Climatic

1004   variability in the northern sector of the American tropics since the latest MIS3. *Quaternary*

1005   *Research,* **84:** 262-271.

1006

1007   Martens K. 1994. Summary of the morphology, taxonomy and distribution of *Limnocythere*

1008   *inopinata* (Baird, 1843) (Ostracoda, Limnocytheridae). In; *The evolutionary ecology of*

1009   *reproductive modes in non-marine Ostracoda.* [Horne DJ, Martens K. (Eds.)]. The

1010   University of Greenwich Press: Greenwich; pp. 17-22.

1011

1012   Metcalfe SE. 1990. *Navicula elkab* O. Müller – a species in need of redefinition? *Diatom*

1013   *Research,* **5:** 419-423.

1014

1015   Metcalfe SE, Street-Perrott FA, Brown RB, Hales PE, Perrott RA, Steininger FM. 1989.

1016   Late Holocene Human Impact on Lake Basins in Central Mexico. *Geoarchaeology*, **4**: 119-

1017   141.

1018

1019   Metcalfe SE, Hales PE. 1994. Holocene Diatoms From A Mexican Crater Lake : La

1020   Piscina De Yuriria. *Memoirs of the California Academy of Sciences*, **17:** 501-515.

1021

1022   Metcalfe SE, Street-Perrott FA, O'Hara SL, Hales PE, Perrott RA (1994) The

1023   palaeolimnological record of environmental change: examples from the arid frontier of

1024   Mesoamerica. In: *Environmental Change in Drylands: Biogeographical and*

1025   *Geomorphological Perspectives*. [Millington AC, Pye K. (eds.)]. John Wiley and Sons Ltd:

1026   Chichester; pp.131-145

1027

1028 Metcalfe SE, Davies SJ, Braisby JD, Leng MJ, Newton AJ, Terrett NL, O'Hara SL. 2007.

1029 Long and short-term change in the Patzcuaro Basin, central Mexico. *Palaeogeography*

1030 *Palaeoclimatologyy Palaeoecology,* **247:** 272-295.

1031

1032 Metcalfe SE, Barron JA, Davies SJ. 2015. The Holocene history of the North American

1033 Monsoon: 'known knowns' and 'known unknowns' in understanding its spatial and

1034 temporal complexity. *Quaternary Science Reviews,* **120:** 1-27.

1035

1036 Ordoñez E. 1900. Les volcans du Valle de Santiago. *Memorias de la Sociedad Cientifica*

1037 *Antonio Alzate (Mexico)* **14:** 299-326.

1038

1039 Park LA. 1999. *Late Quaternary environmental change in La Piscina de Yuriria, Central*

1040 *Mexico: evidence from the palaeolimnological record.* Unpublished MRes thesis,

1041 University of Edinburgh.

1042

1043 Park J, Byrne R, Bohnel H, Molina Garza R, Conserva M. 2010. Holocene climate change

1044 and human impact, central Mexico: a record based on maar lake pollen and sediment

1045 chemistry. *Quaternary Science Reviews,* **29:** 618-632.

1046

1047 Patrick R. Reimer C.W. 1966. The diatoms of the United States exclusive of Alaska and

1048 Hawaii. Vol. 1. *The Academy of Natural Sciences of Philadelphia, Philadelphia,*

1049 *Monograph,* **13:** 668 pp.

1050

1051 Patrick, R. & C. W. Reimer, 1975. The diatoms of the United States exclusive of Alaska

1052 and Hawaii. Vol. 2. Part 1. *The Academy of Natural Sciences of Philadelphia, Philadelphia,*

1053 *Monograph,* **13:** 213 pp.

1054

1055 Reimer PJ, Bard E, Bayliss A, Beck JW, Blackwell PG, Ramsey CB, Buck CE, Cheng H,

1056 Edwards RL, Friedrich M, Grootes PM, Guilderson TP, Haflidason H, Hajdas I, Hatte,

1057 C, Heaton TJ, Hoffmann DL, Hogg AG, Hughen KA, Kaiser KF, Kromer B, Manning SW,

1058 Niu M, Reimer RW, Richards DA, Scott EM, Southon JR, Staff RA, Turney CSM, van der

1059 Plicht J. 2013. Intcal13 and Marine13 Radiocarbon Age Calibration Curves 0-50,000 Years

1060 Cal BP. *Radiocarbon,* **55:** 1869-1887.

1061

1062 Roy PD, Caballero M, Lozano R, Pi T, Morton O. 2009. Late Pleistocene-Holocene

1063 geochemical history inferred from Lake Tecocomulco sediments, Basin of Mexico, Mexico.

1064 *Geochemical Journal*, **43:** 49-64.

1065

1066 Roy PD, Quiroz-Jimenez JD, Perez-Cruz L, Lozano-Garcia S, Metcalfe SE, Lozano-

1067 Santacruz R, Lopez-Balbiaux N, Sanchez-Zavala JL, Romero FM. 2013. Late Quaternary

1068 paleohydrological conditions in the drylands of northern Mexico: a summer precipitation

1069 proxy record of the last 80 cal ka BP. *Quaternary Science Reviews,* **78:** 342-354.

1070

1071 Schoeman FR, Archibald REM. 1977. *The Diatom Flora of South Africa,* Nos. 1-6. CSIR

1072 Special Report WAT 50. Pretoria.

1073

1074 Sears PB, Clisby K. 1955. Palynology in southern North america, Part IV: Pleistocene

1075 climate in Mexico. *Bulletin of the Geological Society of America,* **66:** 521-530.

1076

1077 Talbot MR. 1990. A review of the palaeohydrological interpretation of carbon and oxygen

1078 isotope ratios in primary lacustrine carbonates. *Chemical Geology (Isotope Geosciences*

1079 *Section)*, **80**: 261-279.

1080

1081 Tarutani T, Clayton RN, Mayeda TK 1969. The effect of polymorphism and magnesium

1082 substitution on oxygen isotope fractionation between calcium carbonate and water.

1083 *Geochimica et Cosmochimica Acta,* 33, 987–996.

1084

1085 ter Braak CJF. 1988a. CANOCO - a FORTRAN program for canonical community

1086 ordination by [partial] [detrended] [canonical] correspondence analysis, principal

1087 components analysis and redundancy analysis (version 2.1). Report LWA-88-02.

1088 Agricultural Mathematics Group: Wageningen.

1089

1090 Van Meerbeeck CJ, Renssen H, Roche DM. 2009. How did Marine Isotope Stage 3 and

1091 Last Glacial Maximum climates differ? – perspectives from equilibrium simulations.

1092 *Climate of the Past,* **5**: 33-51.

1093

1094 Vazquez-Selem L, Heine, K. 2004 Late Quaternary glaciation in Mexico. In: *Quaternary*

1095 *Glaciations – Extent and Chronology. Part III South America, Asia, Africa, Australia,*

1096 *Antarctica.* [Ehlers J, Gibbard P. (Eds.)] Elsevier: Amsterdam; pp. 233-242.

1097

1098 von Grafenstein U, Erlernkeuser H, Trimborn P. 1999. Oxygen and carbon isotopes in

1099 modern fresh-water ostracod valves: assessing vital offsets and autecological effects of

1100 interest for palaeoclimate studies. *Palaeogeography Palaeoclimatology Palaeoecology*,

1101 **148**: 133-152.

1102

1103 Watts WA, Bradbury JP 1982. Late Pleistocene and Holocene paleoenvironments and

1104 human activity in the West-Central Mexican Plateau - evidence from Lake Pátzcuaro,

1105 Michoacán, and from the Cuenca de Mexico. *Quaternary Research*, **17**: 56-70.
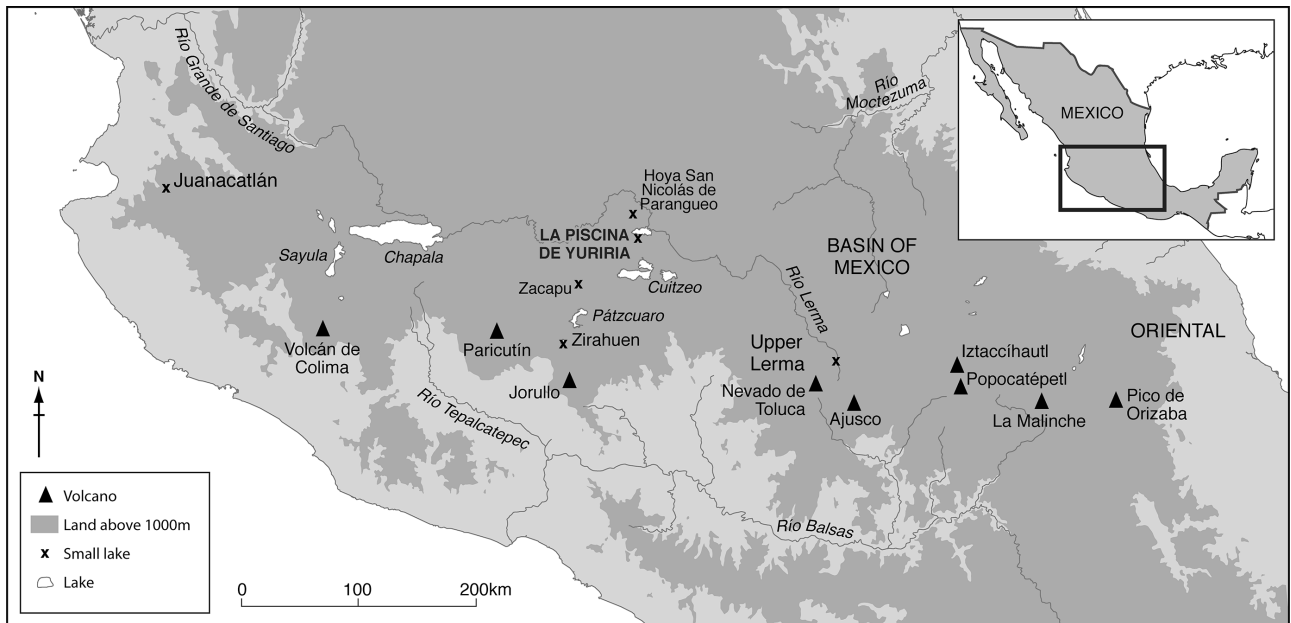
1106

1107   Wolff EW, Chappellaz J, Blunier T, Rasmussen SO, Svensson A. 2010. Millennial-scale

1108   variability during the last glacial: the ice core record. *Quaternary Science Reviews,* **29**:
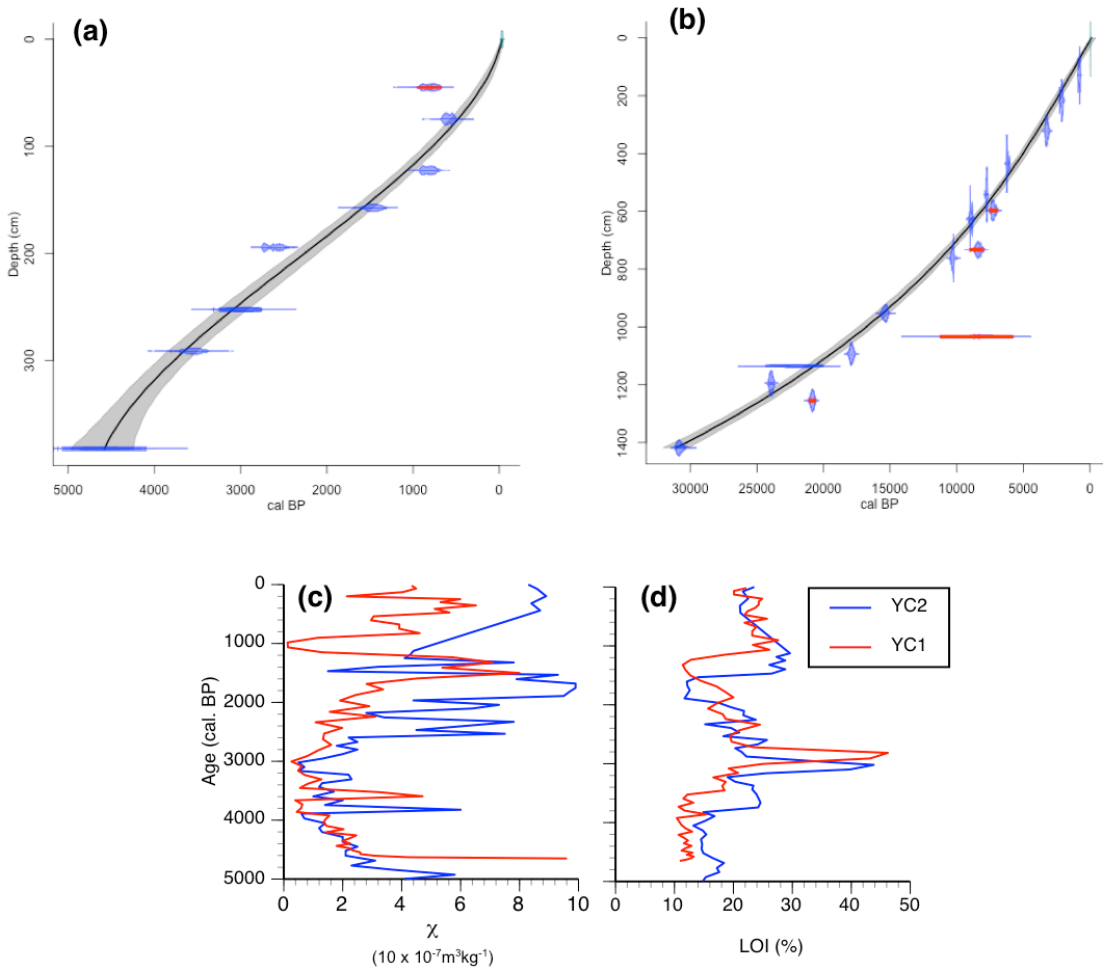
1109   2828-2838.

1110

1111

1112   **Figures**

1114   Fig. 1. Location of la Piscina de Yuriria and other sites referred to in the text.

Fig. 2. Age-depth relationships for (a) YC1 (b) YC2, based on radiocarbon dates. The datapoints are well described by 3rd order polynomial curves, AGE = -0.0001Depth^3 + 0.06645Depth^2 + 2.473Depth – 29.23 for YC1 and, AGE = -0.000005Depth^3 - 0.0006Depth^2 + 12.23Depth – 109.1 for YC2 where age is in calendar years BP and depth is in cm in both cases. Detailed synchronisation for YC1 and the upper part of YC2 based on (c) loss-on-ignition and (d) magnetic susceptibility.
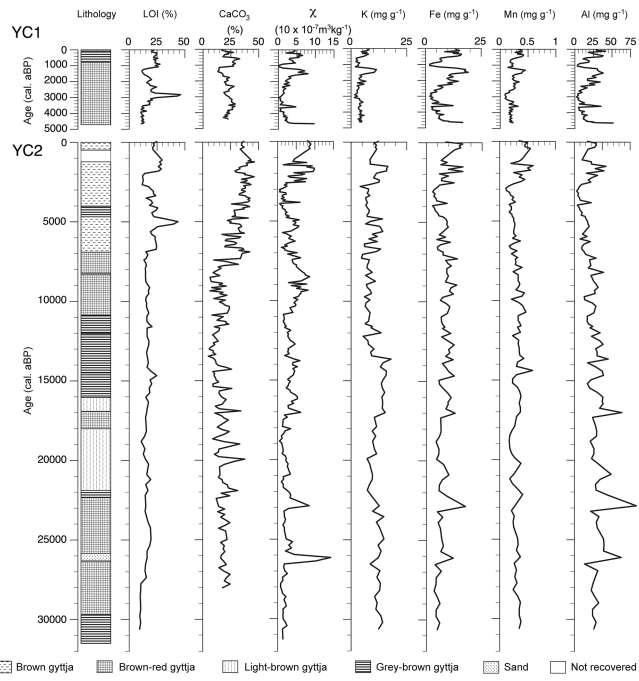
1122

1123   Fig 3. Physical sedimentology and selected elemental geochemical variables for YC1 and

1124   YC2, plotted as a function of age in calendar years.
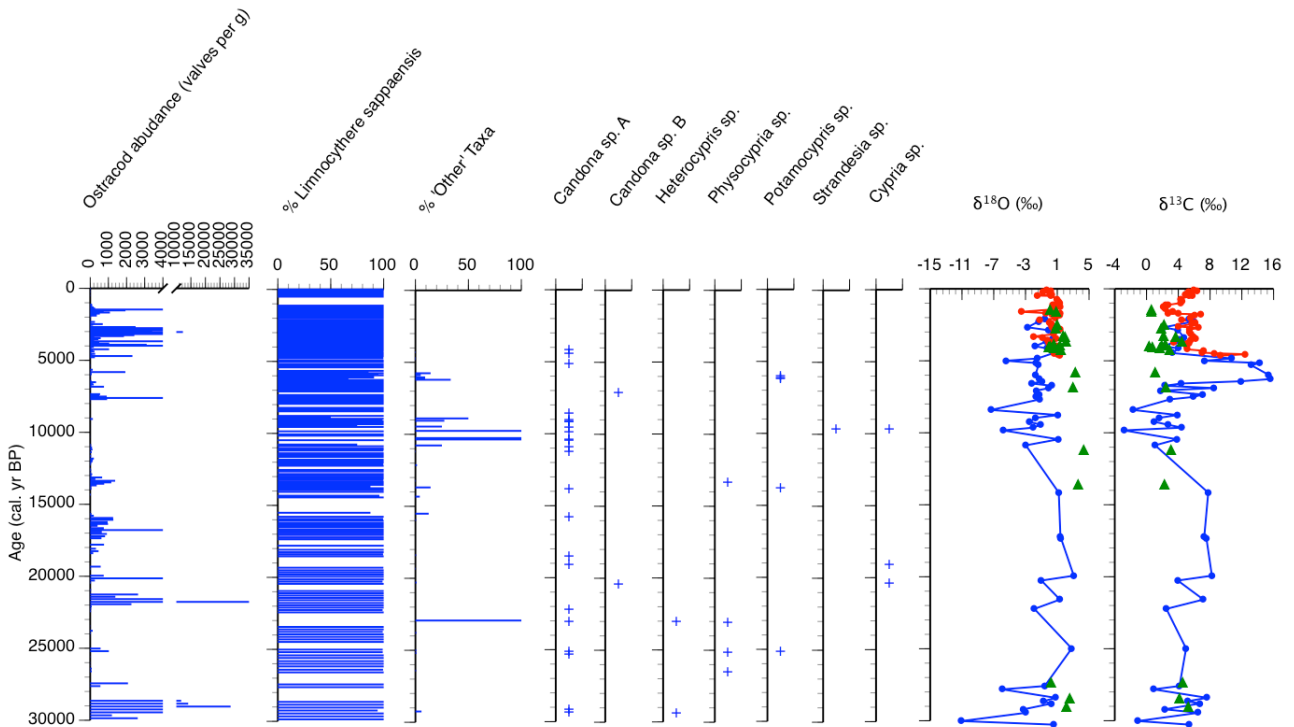
1125

1126   Fig. 4. Ostracod assemblages for YC2 and stable isotopes: endogenic carbonate for YC1

1127   and YC2 and ostracod shells (triangles) for YC2. The 'other taxa' percentage curve

1128   includes all taxa except *Limnocythere sappaensis*.

1129
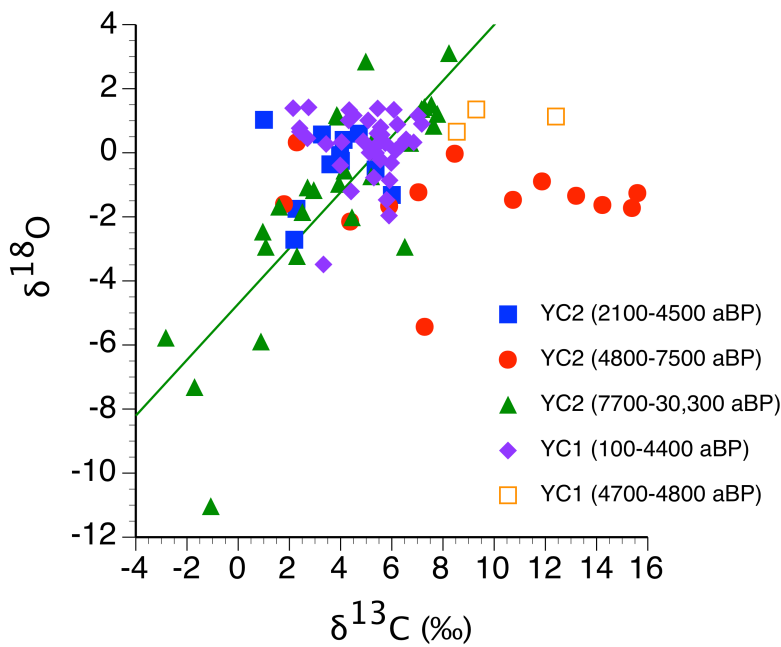
1130

1131 Fig. 5. Covariance of $\delta^{18}O_{carb}$ and $\delta^{13}C_{carb}$ values for YC1 and YC2. For the interval YC2

1132 7700-30,300 aBP only, there is significant covariance between $\delta^{18}O_{carb}$ and $\delta^{13}C_{carb}$ values

1133 (R^2 = 0.68).
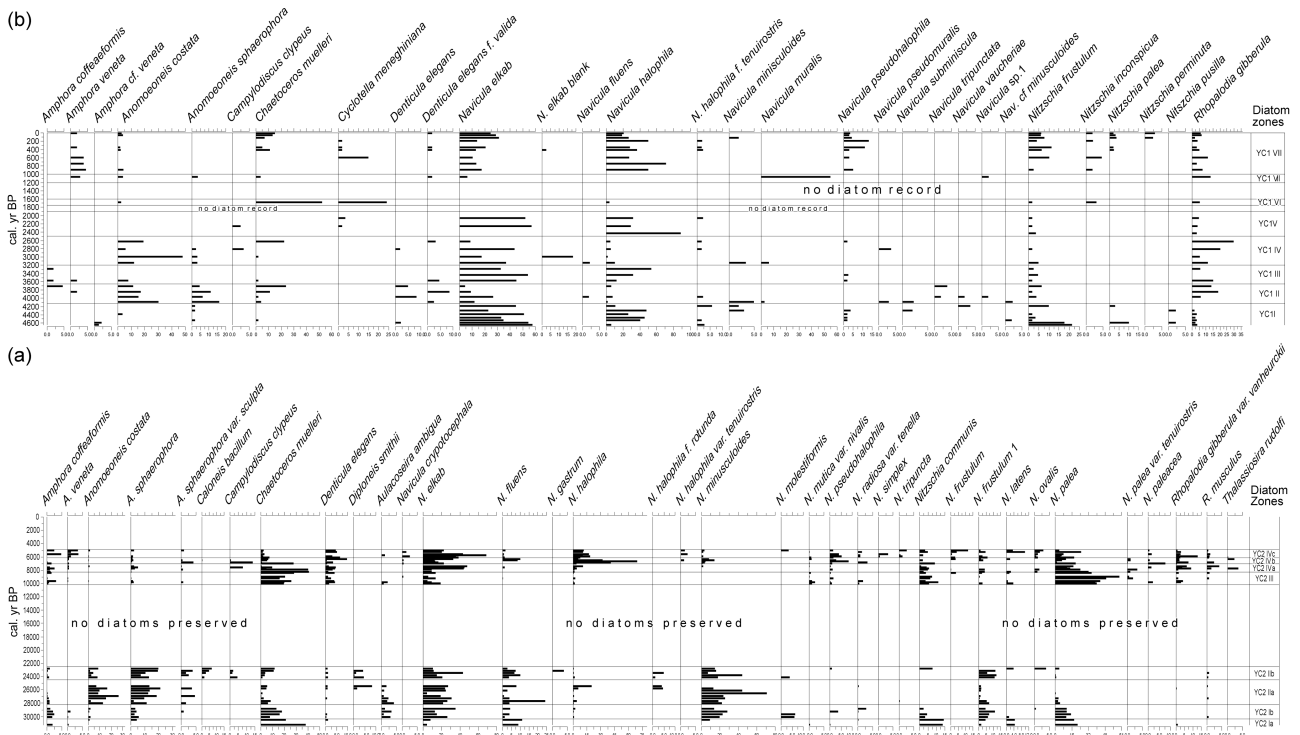
1134

1135 Fig. 6. Diatom abundance (%) for (a) YC2 and (b) YC1. Only taxa present at > 2% and in

1136 more than one sample are plotted.

Fig. 7. Ostracod abundance and magnetic susceptibility for the last 10,000 years in core YC2.
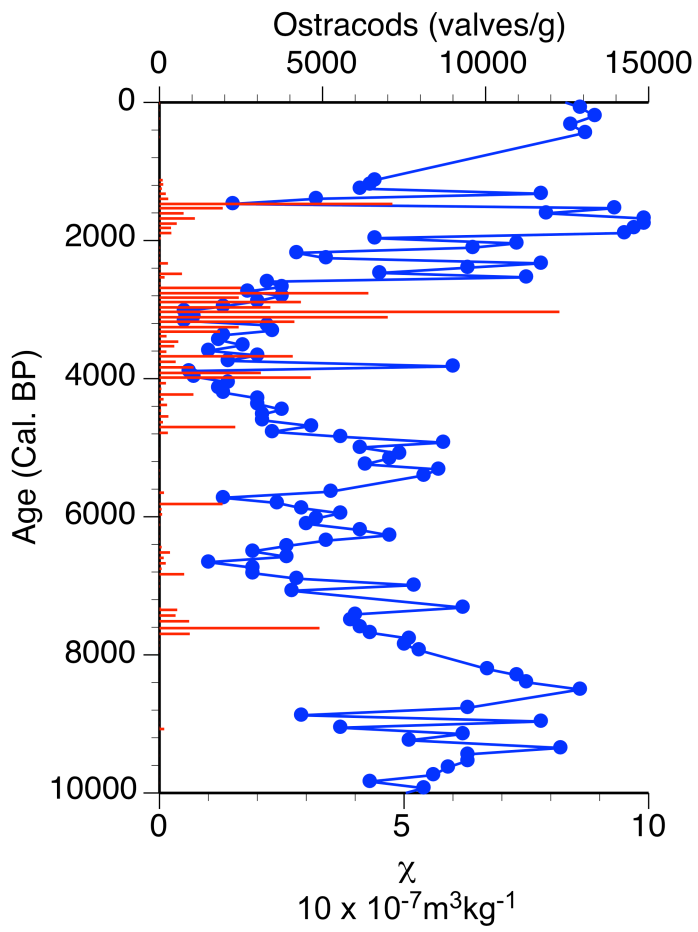
1137

1138 Fig. 7. Ostracod abundance and magnetic susceptibility for the last 10,000 years in core

1139 YC2.

1140

1141

1142

1143

1144

1145

1146

1147

1148

1149

Tables

Table 1. Radiocarbon dates from cores YC1 and YC2.

Table 1. Radiocarbon dates from cores YC1 and YC2

Core	Depth (cm)	Date Type	Lab number	Radiocarbon age (yr)	Error (yr)	Cal age range (yr) (95 % confidence intervals)		Material	Notes
YC1	44-46	AMS	OxA-1963	875	90	670	951	carbonate	omitted from age model
YC1	74-75	AMS	OxA-1964	570	80	500	673	carbonate	
YC1	122-123	AMS	OxA-1965	900	60	705	927	carbonate	
YC1	157-158	AMS	OxA-1966	1570	80	1307	1680	carbonate	
YC1	194-195	AMS	OxA-1967	2540	60	2383	2759	carbonate	
YC1	250-255	AMS	RIDDL-62	2840	120	2751	3323	carbonate	
YC1	291-292	AMS	OxA-1968	3320	90	3372	3824	carbonate	
YC1	380-385	AMS	RIDDL-63	4100	200	4084	5278	carbonate	
YC2	129-130	AMS	AA13908	860	50	689	908	bulk organic carbon	
YC2	216-217	AMS	AA13907	2125	50	1955	2306	bulk organic carbon	
YC2	321-322	AMS	AA13906	3040	70	3008	3391	bulk organic carbon	
YC2	430-440	Radiometric	SRR-5189	5410	50	6018	6300	bulk organic carbon	
YC2	537-547	Radiometric	SRR-5190	6925	45	7670	7911	bulk organic carbon	
YC2	592-602	Radiometric	2815-Ors	6340	140	6939	7552	bulk organic carbon	omitted from age model
YC2	622-632	Radiometric	SRR-5191	8055	50	8730	9120	bulk organic carbon	
YC2	728-738	Radiometric	2844-Ors	7570	188	8001	8967	bulk organic carbon	omitted from age model
YC2	761-762	AMS	AA13905	9105	80	9969	10511	bulk organic carbon	
YC2	953-954	AMS	AA13904	12865	105	15085	15728	bulk organic carbon	
YC2	1029-1039	Radiometric	2812-Ors	7100	1200	5752	11244	carbonate	omitted from age model
YC2	1093-1094	AMS	AA13903	14705	105	17617	18165	bulk organic carbon	
YC2	1130-1140	Radiometric	2869-Ors	18180	980	19938	24375	bulk organic carbon	
YC2	1190-1200	Radiometric	SRR-5192	19880	75	23676	24160	bulk organic carbon	
YC2	1250-1260	Radiometric	SRR-5193	17275	90	20577	21103	bulk organic carbon	omitted from age model
YC2	1413-1423	AMS	AA16907	26590	280	30308	31189	bulk organic carbon	

1152

1153

1154

1155

1156

1157

1158

1159

1160

1161

1162

1163

1164

1165

Table 2. Summary of climatic and environmental changes at La Piscina de Yuriria over the

past 30,000 years

Table 2. Summary of climatic and environmental changes at La Piscina de Yuriria over the past 30,000 years

Age Range (cal. aBP)	Climatic and environmental conditions	Key evidence
0-4,500	Lower effective mositrue under dier climate regime but with short-lived wetter intervals	Oxygen isotopes
	Saline -alkaline lake	Ostracods, diatoms
	Transient anthropogenically-induced inwash events associated with catchment instability	Elemental geochemistry and magnetic susceptibility
4,500-8,000	Reduced effective moisture leading to enhanced evaporative enrichment under drier climate	Oxygen isotopes
	Saline - alkaline lake with nutrient enrichment and short-lived fresher interval	Ostracods, diatoms
	Intense methane formation	Carbon isotopes
	Climatically-contorlled inwash event during wet intervals	Elemental geochemistry and magnetic susceptibility
8,000-11,000	Higher effective moisture, but with evidence of variability under wetter but variable climatic regime	Oxygen isotopes
	Fresher and deeper lake, but eutrophic	Ostracods, diatoms
11,000-14,000	Dry climate, lake dessication	Stratography (presence of desiccation surface)
14,000-25,500	Reduced effective moisture leading to enhanced evaporative enrichment under drier climate	Oxygen isotopes
	Periodic lake desiccation	Stratography (presence of desiccation surface)
	Saline - alkaline lake with short-lived fresher intervals	Ostracods, diatoms
	Shallow eutropic lake with methane formation	Diatoms, carbon isotopes
	Stable catchment with limited inwash	Elemental geochemistry and magnetic susceptibility
27,500-30,000	Rapid shifts between low and high effective mositure under variable dry to wet climatic regime, possibly accompanied by cooler conditions	Oxygen isotopes
	Saline - alkaline lake	Ostracods, diatoms
	Shallow eutropic lake with methane formation	Diatoms, carbon isotopes
	Stable catchment with limited inwash	Elemental geochemistry and magnetic susceptibility

1168

1169

1170

Supporting online information

1172 Table S1. Water Chemistry for La Piscina de Yuriria. Date from Davies (1995) and various

1173 unpublished sources.

Table S1. Water Chemistry for La Piscina de Yuriria. Date from Davies (1995) and various unpublished sources.

Year	Water depth (m)	Type	pH	EC^ (µScm-1)	Alkalinity (Total) (meqL^{-1})	Cl (meqL^{-1})	SO$_4$ (meqL^{-1})	K (meqL^{-1})	Na (meqL^{-1})	Ca (meqL^{-1})	Mg (meqL^{-1})	TP (µgL^{-1})	δ^{13}C$_{DIC}$ ‰VPDB	δ^{18}O ‰ VSMOW	δD ‰ VSMOW
1982 (April)	2 (surface)	Lake	11.0	26000	300.0	174.3	29.3	30.7	478.5	0.0	0.0	ND$^{\#}$	ND	ND	ND
1982 (April)	2 (at depth)	Lake	NA	23000	326.0	141.5	30.2	24.8	478.5	0.0	0.0	ND	ND	ND	ND
1982 (April)	0.2 (margin)	Lake	11.0	29000	294.0	116.3	29.5	32.1	413.3	0.0	0.0	ND	ND	ND	ND
1982 (April)		Spring	7.5	500	6.2	0.4	1.4	0.6	3.7	1.0	1.3	ND	ND	ND	ND
1982 (April)		Spring	7.0	1100	5.0	1.1	3.6	1.0	9.6	1.1	1.6	ND	ND	ND	ND
1982 (May)	0.2 (margin)	Lake	9.6	27500	333.0	203.0	33.5	32.1	543.7	0.0	0.0	ND	ND	ND	ND
1982 (May)		Spring	7.7	700	8.0	4.2	0.3	0.6	8.9	0.9	1.6	ND	ND	ND	ND
1992 (August)	0.2	Lake	10.5	15620	248.2	117.4	50.0	22.8	298.5	0.3	0.1	ND	-0.2	0.7	-25
1992 (August)		well	6.8	315	3.7	0.4	9.6	0.9	5.7	4.4	3.9	ND	-10.4	-9.2	-69
1992 (August)		spring	8.0	452	7.7	0.4	7.5	2.0	8.4	3.3	3.7	ND	-11.6	-9.1	-69
1997 (March)	shore	Lake	10.2	8130	68.3	27.5	9.2	7.0	95.8	5.9	1.9	ND	ND	ND	ND
2003 (March)	0.2 (margin)	Lake	9.5	1907	20.8	6.2	0.4	1.7	26.3	2.9	2.4	562.0	ND	ND	ND
2004 (July)	0.2 (margin)	Lake	9.6	2910	16.4	16.7	0.8	1.5	163.4*	2.6	0.0	744.5	ND	ND	ND
2003 (March)		Groundwater	8.0	1076	ND	ND	ND	ND	ND	ND	ND	ND	ND	ND	ND

^Electrical conductivity
$^{\#}$ND = not determined
* possible contamination

1174
1175

1176

1177

1178

1179

1180

1181

1182

1183

1184

1185

1186

1187

1188

1189

1190 Table S2. Correlation matrices (R^2 values) for correlation amongst selected geochemical

1191 variables from (a) YC1 (b) YC2, whole core (c) YC2 post 5000 aBP. In each table the null

1192 hypothesis (H_o) is that there is no statistically-significant relationship between the two

1193 variables

Table S2. Correlation amongst selected geochemical variables

(a) Core YC1

		K	Fe	Mn	Al
K	R^2	1.			
	p-value				
	H0 (5%)				
Fe	R^2	0.65	1.		
	p-value	1.68E-16			
	H0 (5%)	rejected			
Mn	R^2	0.68	0.77	1.	
	p-value	8.35E-18	0.00E+00		
	H0 (5%)	rejected	rejected		
Al	R^2	0.52	0.901	0.67	1.
	p-value	4.76E-12	0.00E+00	2.46E-17	
	H0 (5%)	rejected	rejected	rejected	

(b) Core YC2 - all

		K	Mn	Fe	Al
K	R^2	1.			
	p-value				
	H0 (5%)				
Fe	R^2	0.15	1.		
	p-value	0.00001			
	H0 (5%)	rejected			
Mn	R^2	0.06	0.45	1.	
	p-value	0.00581	4.00E-17		
	H0 (5%)	rejected	rejected		
Al	R^2	0.22	0.19	0.37	1.
	p-value	4.32E-08	6.67E-07	0.	
	H0 (5%)	rejected	rejected	rejected	

(b) Core YC2 - post 5000 aBP

		K	Mn	Fe	Al
K	R^2	1.			
	p-value				
	H0 (5%)				
Fe	R^2	0.61	1.		
	p-value	9.64E-08			
	H0 (5%)	rejected			
Mn	R^2	0.49	0.75	1.	
	p-value	5.96E-06	7.15E-11		
	H0 (5%)	rejected	rejected		
Al	R^2	0.59	0.71	0.8	1.
	p-value	2.00E-07	9.10E-10	1.67E-12	
	H0 (5%)	rejected	rejected	rejected	

1194

1195

1196

1197